ACS chemical biology

Articles

pubs.acs.org/acschemicalbiology

A Novel Small Molecule Methyltransferase Is Important for Virulence in *Candida albicans*

Elena Lissina,[†] David Weiss,[‡] Brian Young,[‡] Antonella Rella,[§] Kahlin Cheung-Ong,[†] Maurizio Del Poeta,[§] Steven G. Clarke,[‡] Guri Giaever,[∥] and Corey Nislow*[,∥]

[†]Department of Molecular Genetics, Terrence Donnelly Centre for Cellular and Biomolecular Research, University of Toronto, 160 College St., Toronto, M5S 3E1, Canada

[‡]Department of Chemistry and Biochemistry and the Molecular Biology Institute, University of California, 607 Charles E. Young Drive East, Los Angeles, California 90095-1569, United States

[§]Department of Molecular Genetics and Microbiology, Stony Brook University, 150 Life Sciences Building, Stony Brook, New York 11794-5222, United States

[∥]Department of Pharmaceutical Sciences, University of British Columbia, 2405 Wesbrook Mall, Vancouver, BC V6T 1Z3, Canada

Supporting Information

ABSTRACT: *Candida albicans* is an opportunistic pathogen capable of causing life-threatening infections in immunocompromised individuals. Despite its significant health impact, our understanding of *C. albicans* pathogenicity is limited, particularly at the molecular level. One of the largely understudied enzyme families in *C. albicans* are small molecule AdoMet-dependent methyltransferases (smMTases), which are important for maintenance of cellular homeostasis by clearing toxic chemicals, generating novel cellular intermediates, and regulating intra- and interspecies interactions. In this study, we demonstrated that *C. albicans* Crg1 (CaCrg1) is a *bona fide* smMTase that interacts with the toxin *in vitro* and *in vivo*. We report that CaCrg1 is important for virulence-related processes such as adhesion, hyphal elongation, and membrane trafficking. Biochemical and genetic analyses showed that CaCrg1 plays a role in the complex sphingolipid pathway: it binds to exogenous short-chain ceramides *in vitro* and interacts genetically with genes of glucosylceramide pathway, and the deletion of *CaCRG1* leads to significant changes in the abundance of phytoceramides. Finally we found that this novel lipid-related smMTase is required for virulence in the waxmoth *Galleria mellonella*, a model of infection.

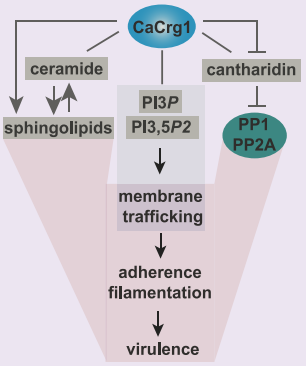

The fungus *Candida albicans* is a normally harmless commensal present in the human gastrointestinal tract. However, this fungus can cause life-threatening infections in immunocompromised individuals.[1,2] Our current understanding of *Candida*'s pathogenicity mechanisms is incomplete. According to the *Candida* Genome database (www.candidagenome.org) over 70% of *C. albicans* genes are annotated as uncharacterized, and much of the current characterization relies on homology to genes in the model yeast *Saccharomyces cerevisiae*.

One of the poorly studied enzyme families in *C. albicans* are *S*-adenosylmethionine (AdoMet)-dependent MTases. Small molecule MTases (smMTase) are of particular interest, because they are involved in biotransformation of endogenous as well as exogenous small molecules (lipids, xenobiotics, and secondary metabolites) and they maintain cellular homeostasis by clearing toxic chemicals, generating cellular intermediates, and regulating intra- and interspecies interactions.[3−6] Considering the importance of smMTases in response to small molecules, the characterization of these enzymes in *C. albicans* will enhance our understanding of the fungal drug response and may provide a starting point for the development of novel antifungal drugs. Small molecule MTase have been refractory to interrogation because many of these enzymes do not have an obvious phenotype in standard laboratory conditions, and biochemical strategies designed for protein MTases[7,8] are not effective for smMTases because these tests rely on prior knowledge of substrates. Computational analysis can predict functions for smMTases,[3,7,9] yet experimental approaches are required to determine the cellular ligands of smMTases.

We previously used a chemical genetics approach in *S. cerevisiae* to identify an AdoMet-dependent MTase *CRG1* as a gene dose-dependent interactor of cantharidin.[10,11] Cantharidin is a secondary metabolite, produced by blister beetles of the Meloidae family. It functions as a precopulatory agent and is also suggested to act as a protection for beetle eggs.[12,13] Humans have used this natural product as aphrodisiac (aka Spanish fly), as a topical therapy for warts and tattoo removal, and to treat hepatocellular carcinoma in traditional Chinese medicine.[14] Additionally, cantharidin analogues are currently being investigated as anticancer therapies.[15]

Received: August 13, 2013
Accepted: October 1, 2013
Published: October 1, 2013

The primary targets of cantharidin are type I and type II protein phosphatases,[16,17] yet we showed that cantharidin interacts with the MTase Crg1 *in vitro* and that Crg1 maintains lipidome homeostasis in non-pathogenic fungi.[11] In *C. albicans* putative MTase *orf19.633* is also a gene-dose modulator of the cantharidin response. At the primary sequence level *ScCRG1* and *CaCRG1* have limited homology within their putative MTase domains (19.2% identity and 38.5% similarity), indicating that the function of *orf19.633* in its response to the toxin could not be inferred solely from its sequence. Despite this evolutionary divergence, our functional tests show that CaCrg1 robustly rescues a *Saccharomyces crg1* deletion mutant. BLASTp analysis reveals that *CaCRG1* shares homology with other human fungal pathogens genes with unknown functions: *Candida dubliniensis* (*CD36_30360*, 77.9% identity, 85.2% similarity), *Candida tropicalis* (*CTRG_00537*, 65.4% identity, 80.3% similarity), *Candida parapsilosis* (*CPAR2_204610*, 57.9% identity, 74.3% similarity), *Candida orthopsilosis* (*CORT_0D04720*, 57.8% identity, 74% similarity). Given the rise in non-*albicans* infections[18] these observations suggest that the study of CaCrg1 can provide insight into these related pathogens.

Here we used cantharidin as a small molecule probe to characterize *CaCRG1* in *C. albicans*. Our biochemical and genetic analysis provides evidence that CaCrg1 is a lipid-binding smMTase essential for cellular defense against chemical stress and for maintenance of virulence-related processes in the response to cantharidin. We also demonstrated that *CaCRG1* is important for virulence of *C. albicans* in the waxworm *Galleria mellonella*.

RESULTS AND DISCUSSION

A Functional CaCrg1 Is Important for Cantharidin Resistance. The aim of this work was to characterize a putative MTase *orf19.633* (*CaCRG1*) and uncover biological functions for this enzyme. *Orf19.633* (hereafter CaCrg1) was annotated as a MTase having AdoMet-binding motifs.[10,11] To test if it is a functional MTase, we synthesized a codon-optimized *CaCRG1* sequence (Bio Basic Inc.) and expressed it in *S. cerevisiae* (Supplementary Figure 1A). The synthesized gene was further used as a template to produce mutant alleles (D48A, E153A-R156G, and motif IIIΔ), using *S. cerevisiae crg1*Δ/Δ null mutant as the expression host. Galactose-induced overexpression of wild type (wt) *CaCRG1* completely rescued *crg1*Δ/Δ sensitivity to cantharidin, whereas the mutant alleles (D48A and Motif IIIΔ) failed to confer cantharidin resistance (Figure 1). The failure to complement was not due to reduced expression of the mutated CaCrg1 proteins (Supplementary Figure 1B), indicating that the MTase domain of CaCrg1 is both necessary and sufficient for cellular survival in cantharidin.

Cantharidin Is Methylated by CaCrg1. Because CaCrg1 is required for cantharidin resistance, we tested if CaCrg1 catalyzes a methylation reaction on cantharidin similar to that of ScCrg1.[10,11] We purified the *Candida* enzyme expressed in baker's yeast (Figure 2A) and found that an acid-hydrolyzed reaction mixture of the purified CaCrg1, cantharidin, and *S*-adenosyl-[*methyl*-^{14}C]-L-methionine results in the formation of volatile radioactive methyl ester (as methanol) (Figure 2B). This activity was dependent on the presence of both the protein and cantharidin (Supplementary Figure 2) demonstrating that CaCrg1 is a functional MTase methylating cantharidin *in vitro*.

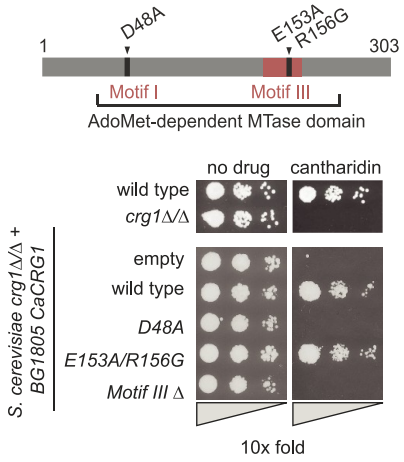

Figure 1. A functional MTase domain of CaCrg1 is required for cantharidin resistance. (Top) Diagram of MTase domain with the point mutations and the deletion of Motif III. (Bottom) Growth of *S. cerevisiae* wt and *crg1*Δ cells overexpressing empty vector *BG1805*, wt, and mutated *CaCRG1* alleles (D48A, E153A/R156G, and Motif IIIΔ) in the presence of cantharidin (80 μM).

To determine if CaCrg1 is required for *in vivo* methylation of cantharidin, we investigated the metabolism of cantharidin in wt and a *cacrg1*Δ/Δ mutant. Mid-exponentially grown cells were treated with cantharidin (100 μM) or DMSO for 90 min. Intracellular metabolites were rapidly extracted and analyzed by liquid chromatography−tandem mass spectrometry (LC−MS/MS). In the m/z = 197 single-ion chromatogram, we observed the peak corresponding to cantharidin (m/z = 197) in wt and *cacrg1*Δ/Δ cells grown in the presence of the drug (Figure 2C, left panel). These chromatographic peaks eluting at 19.4 min with m/z ratios matching cantharidin were absent in cells treated only with DMSO. Next, we examined the m/z = 211 single-ion chromatogram, which corresponds to the mass range of methyl cantharidin (m/z = 211) (Figure 2C, right panel). We observed a large peak eluting at 19.9 min in wt cells treated with cantharidin in the mass range matching methylated cantharidin. In contrast, no peak in this mass range was observed in cantharidin-treated *cacrg1*Δ/Δ cells or in cells treated with DMSO alone. The spectra of the 19.4-min cantharidin peak in the drug-treated wt cells corresponded to cantharidin (m/z = 197) and cantharidin water adduct or hydrated cantharidin derivative (m/z = 215) (Figure 2D, left panel). When we analyzed the spectra of the CaCrg1-dependent 19.9-min methyl cantharidin peak in the drug-treated wt, we saw ions corresponding to methyl cantharidin (m/z = 211), hydrated methyl cantharidin (m/z = 229), and unmodified cantharidin (m/z = 197), a possible product of in-source fragmentation (Figure 2D, right panel). Our findings indicate that cantharidin is methylated *in vivo* in *C. albicans* and that CaCrg1 is the small molecule AdoMet-dependent MTase responsible for this activity.

***CaCRG1* Is Important for *Candida* Morphogenesis in Response to the Drug.** Despite its long history of use, the antifungal activity of cantharidin has not been characterized in detail.[19] To define its molecular mechanism in *C. albicans*, we profiled its transcriptional response using gene expression arrays (stCANDIDA 1a). Exponentially grown cells were treated with cantharidin at its IC_{50} (2 mM) in YPD or DMSO for 30 min. Transcriptome analysis revealed 235 differentially expressed genes ($\log_2$ (cantharidin/DMSO) < |2|,

dx.doi.org/10.1021/cb400607h | *ACS Chem. Biol.* 2013, 8, 2785−2793

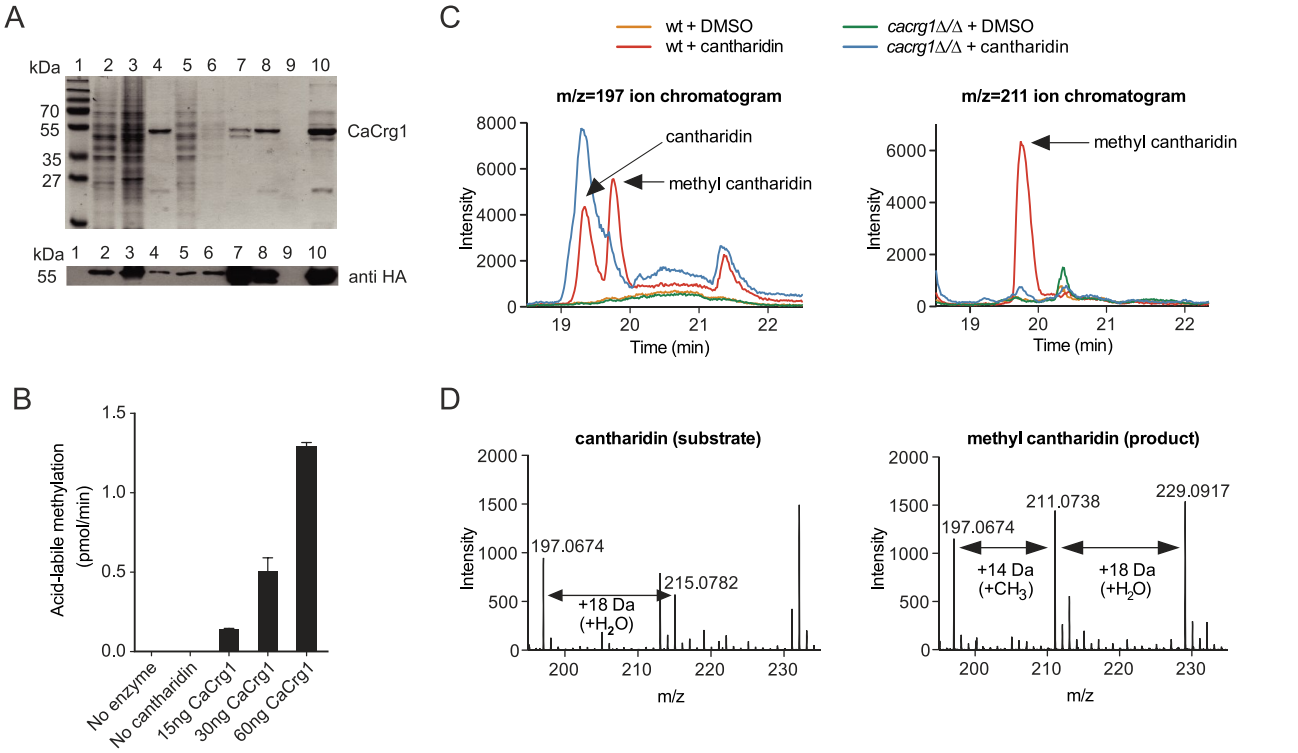

Figure 2. CaCrg1 is a small molecule MTase. (A) Coomassie-stained 12% SDS-PAGE of purified His-tagged CaCrg1. Lane 1, molecular weight standards; lane 2, soluble cell extract; lane 3, insoluble fraction; lane 4, Ni^{2+} Sepharose beads after wash 1; lane 5, unbound to beads cell extract; lane 6, wash 1; lane 7, beads after three washes; lane 8, nonconcentrated elute; lane 9, flow-through; lane 10, concentrated and desalted elute. The expression of CaCrg1 was assessed with a mouse monoclonal anti-HA antibody (bottom). (B) CaCrg1 shows robust MTase activity with cantharidin as the substrate *in vitro*. The reactions containing varying amounts of CaCrg1 enzyme and cantharidin were tested on production acid-labile methylated ester. The error bars represent the standard deviation of two separate experiments each performed in duplicate. (C) CaCrg1 is required for a formation of methyl cantharidin *in vivo*. Wt and *cacrg1*Δ/Δ cells were cultured in the presence and absence of cantharidin before extraction of intracellular metabolites and analysis by LC−MS/MS. Single-ion chromatograms of various cellular extracts are shown for the mass ranges corresponding to cantharidin (m/z = 197 ± 100 ppm) (left panel) and methyl cantharidin (m/z = 211 ± 100 ppm) (right panel). Arrows mark the elution patterns for cantharidin and methyl cantharidin. (D) Averaged spectra of the cantharidin (left panel) and methyl cantharidin (right panel). Chromatographic peaks from the cantharidin-treated wt are shown, and ions of interest are indicated.

P-value < 0.05; Figure 3A and Supplementary Table 1), 91% of which were downregulated. These genes were significantly enriched in the Gene Ontology (GO) term processes "cell adhesion" (*P*-value < 8.65×10^{-4}), "positive regulation of response to stimulus" (*P*-value < 2.37×10^{-2}), and "regulation of filamentous growth" (*P*-value < 3.6×10^{-2}). *CaCRG1* was among the significantly upregulated genes ($\log_2 > 2.3$, *P*-value < 9.0×10^{-4}), and qRT-PCR analysis confirmed that the relative abundance of *CaCRG1* transcript increases in the response to cantharidin in a time-dependent manner (Figure 3B). Because cantharidin is a potent protein phosphatase inhibitor,[17] its effects on gene expression are likely due to interfering with phosphorylation-dependent signaling.

Because cantharidin treatment leads to downregulation of genes involved in two phenotypes that are directly related to *C. albicans* virulence (adhesion and filamentation),[20] we assessed these phenotypes in *cacrg1*Δ/Δ mutant in the presence of the drug. *Cacrg1*Δ/Δ showed reduced adherence to plastic (*P*-value <1.0×10^{-3}; Figure 3C and Supplementary Figure 3) and completely failed to adhere to plastic in the presence of non-growth inhibitory doses of cantharidin (10 μM) (*P*-value < 8.0×10^{-10}). The mutant also failed to germinate when exposed to a non-growth inhibitory dose (10 μM) (Figure 3D), whereas under standard conditions (without the drug at 37 °C) *cacrg1*Δ/Δ underwent hyphal elongation similarly to wt. These results indicate that cantharidin treatment affects germination of fungi and CaCrg1 is required to maintain fungal morphogenesis in response to the drug.

CaCrg1Maintains Membrane Trafficking during Cantharidin Exposure. Because we previously found that cantharidin treatment affected the formation of actin patches[11] (the sites of endocytosis in *S. cerevisiae*), we tested if endocytosis is perturbed by the drug in *C. albicans*. Using the lipophilic styryl dye FM4-64 to follow the dynamics of membrane internalization and transport *via* endosomal intermediates to the vacuole,[21] we found that cantharidin interferes with endocytosis or membrane trafficking in a *cacrg1*Δ/Δ mutant (Figure 4A). After 15 min of cantharidin treatment (250 μM), both wt and the mutant demonstrated brightly stained plasma membrane and vacuolar membranes. Within 60 min of the drug exposure, wt had exclusively vacuolar membrane staining (Figure 4A), whereas in *cacrg1*Δ/Δ mutants the plasma membrane staining remained as small puncta and vacuoles were enlarged. Because the endosome system is essential for trafficking of membrane components (*e.g.*, lipids) and is a point of sorting cargo either for degradation or recycling it back to plasma membrane, our observations suggest that CaCrg1 is important for membrane trafficking in response to cantharidin. Consistent with this finding, CaCrg1 also preferentially binds *in vitro* to established biomarkers of early and late endosomes (Supplementary Figure 4A), the membrane phosphoinositides phosphatidylinositol

dx.doi.org/10.1021/cb400607h | *ACS Chem. Biol.* 2013, 8, 2785−2793

A

Upregulated Genes (18)

ORF	GENE	Log2	P-value
orf19.6475		7.47	1.00E-04
orf19.1048	IFD6	7.44	5.71E-03
orf19.4173	DPH2	6.91	4.34E-03
orf19.2713	MSH5	6.69	3.55E-03
orf19.5604	MDR1	6.30	3.47E-03
orf19.629	IFD7	6.00	1.50E-03
orf19.3848		5.08	9.22E-03
orf19.4309	GRP2	4.49	1.20E-04
orf19.7296		4.39	3.19E-03
orf19.2451	PGA45	4.02	4.31E-03
orf19.3735		3.64	1.00E-03
orf19.4477	CSH1	3.47	1.57E-03
orf19.2023	HGT7	2.96	2.30E-02
orf19.7085		2.75	1.16E-02
orf19.633	CaCRG1	2.30	9.05E-04
orf19.251		2.19	2.74E-03
orf19.5806	ALD5	2.13	3.36E-03
orf19.4631	ERG251	2.11	6.86E-03

Downregulated Genes (196)

GO TERM	P- value
GO:0007155 cell adhesion	8.65E-04
GO:0048584 positive regulation of response to stimulus	2.37E-02
GO:0010570 regulation of filamentous growth	3.62E-02

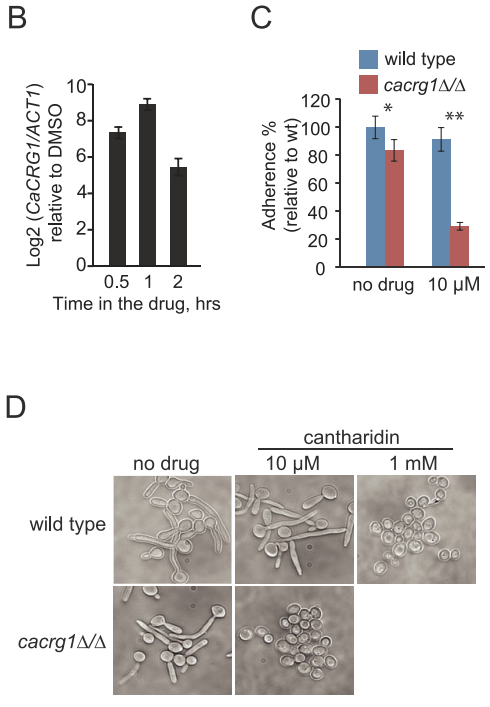

Figure 3. *CaCRG1* is important for cantharidin-perturbed morphogenesis and membrane trafficking in *C. albicans*. (A) Transcriptional profile of wt grown in the presence of cantharidin. GO Biological Term Enrichment was applied to significantly (*P*-value < 0.05) downregulated genes (log_2 (drug/DMSO) > |2|). (B) qRT-PCR analysis demonstrates that *CaCRG1* is a cantharidin-responsive gene. Data are means of at least three independent experimental replicates, and error bars are SD. (C) *cacrg1*Δ/Δ has reduced adherence to plastic surface in the presence and absence of cantharidin. **P*-value < 0.05, ***P*-value < 0.01. (D) *cacrg1*Δ/Δ fails to form hyphae in the presence of cantharidin.

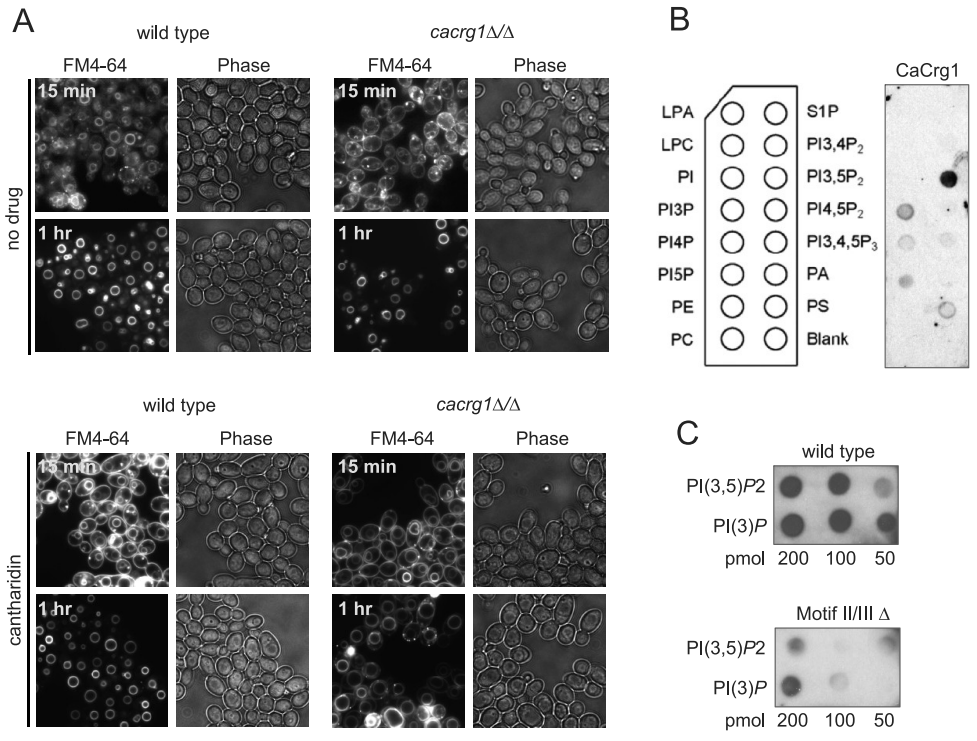

Figure 4. CaCrg1 maintains membrane trafficking during cantharidin exposure. (A) Visualization of endosome dynamics in wt and *cacrg1*Δ/Δ after 15 and 60 min in the presence and absence of cantharidin. (B) Lipid−protein overlay assay of CaCrg1. Lipids: lysophosphatidic acid (LPA), lysophosphocholine (LPC), phosphatidylinositol (PtdIns), PtdIns phosphate (PI(n)P), phosphatidylethanolamine (PE), phosphatidylcholine (PC), sphingosine-1-phosphate (S1P), phosphatidic acid (PA), phosphatidylserine (PS). (C) Validation of the lipid-overlay experiment with PI(3)*P* and PI(3,5)*P*2.

phosphate PI(3)*P* and phosphatidylinositol bisphosphate PI(3,5)*P*2,[22,23] and the binding was dependent on the MTase domain of CaCrg1 (Figure 4B and C). In the baker's yeast we found that in addition to its cytoplasmic distribution GFP-

dx.doi.org/10.1021/cb400607h | *ACS Chem. Biol.* 2013, 8, 2785−2793

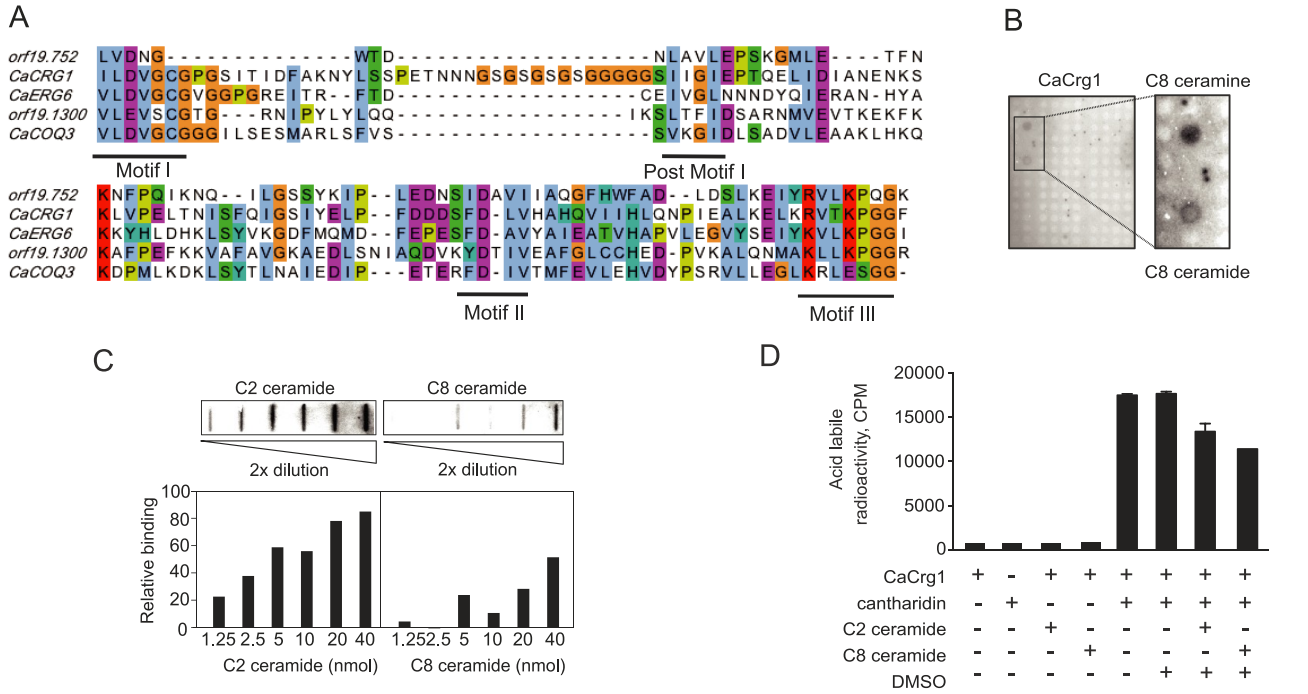

Figure 5. CaCrg1 binds short-chain ceramides *in vitro*. (A) Alignment of protein sequences of CaCrg1MTase domain and its closest homologues. The protein sequences are aligned using the MUSCLE software with the EMBL-EBI Alignment program. Conserved motifs in the MTase domain are underlined. (B) CaCrg1 binds to C8-ceramide and C8-ceramine molecules *in vitro*. (C) Lipid-CaCrg1 overlay assay with biologically active ceramide analogues (C2- and C8-ceramides spotted on the nitrocellulose membrane. Quantification of relative binding of CaCrg1 to ceramides was performed with ImageJ software. (D) The addition of ceramides decreases acid-labile methylation of cantharidin by CaCrg1 *in vitro*.

tagged ScCrg1 is co-localized with the vacuolar membrane (Supplementary Figure 4B). Taken together, our findings suggest that CaCrg1 is involved in fungal morphogenesis and the concomitant changes in membrane trafficking that occur during this shift.

Affinity-Purified CaCrg1 Binds Exogenous Short-Chain Ceramides *in Vitro*. In its MTase domain CaCrg1 demonstrates limited similarity to small molecule MTases, such as *orf19.300* (27.2% identity, 54.3% similarity), *orf19.752* (28% identity, 46.6% similarity), *CaCOQ3* (27.3% identity, 51.2% similarity), and *CaERG6* (28% identity, 44.1% similarity) (Figure 5A). Having established that CaCrg binds to membrane lipids and has partial homology to lipid-related MTases, we tested whether CaCrg1 interacts with bioactive lipids. Accordingly, we prepared a microarray comprising 195 bioactive lipids (Supplementary Table 2) and assessed binding of CaCrg1 by a lipid-overlay assay. We found that purified CaCrg1 binds specifically to C8-ceramide (*N*-octanoylsphingosine) and its analogue C8-ceramine (*N*-octylsphingosine) (Figure 5B and C). CaCrg1 also binds to C2-ceramide and does not bind to C16-ceramide (*N*-palmitoylsphingosine) and other sphingolipid species (Supplementary Figure 5A and 5B). Although the binding of CaCrg1 to ceramides is of particular interest (because these bioactive molecules are involved in stress response, cell growth, senescence, apoptosis, and autophagy[24]), these results must be interpreted with caution because endogenous short-chain ceramides (C2, C6, and C8) have not been found in yeast, and thus the biological relevance of this binding *in vitro* remains to be determined. We also observed that co-incubation of CaCrg1with C2- and C8-ceramides and cantharidin resulted in significant reduction in the formation of methyl esters in an acid-labile methylation assay (Figure 5D). This suggests that, *in vitro*, short-chain ceramides can compete with cantharidin for the binding site as a substrate. In our mass spectrometry analysis, however, we did not detect the formation of methyl derivatives of ceramides, indicating that in the tested conditions short chain ceramides are not substrates of CaCrg1.

***CaCRG1* Interacts with Genes of the Sphingolipid Biosynthesis Pathway.** Ceramides serve as both bioactive molecules and as structural elements required for the biosynthesis of complex sphingolipids (*e.g.*, glucosylceramides (GlcCer)).[24] Complex sphingolipids, generated by an addition of a sugar group to otherwise cytotoxic ceramides, have been recognized as participatory in host−pathogen interactions.[25−28] Phylogenetic analysis also suggested that CaCrg1 is a putative GlcCer MTase.[29] To investigate the biological significance of the observation that CaCrg1 interacts with ceramides *in vitro* and to test if *CaCRG1* is related to complex sphingolipid biosynthesis, we assessed genetic interactions between *CaCRG1* and GlcCer genes by constructing isogenic double deletion mutants in *C. albicans* with a *cacrg11*Δ/Δ strain. Because genetic interactions between any two genes is a rare event (~0.5%), assessing the fitness of double deletion mutations can yield insight into gene function. For example, if a double mutant is less fit than predicted by the combination of both single mutants (known as synthetic sick or lethal), the genes are likely to act in overlapping pathways or in the same essential pathway.[30] In contrast, positive or suppressive interactions between two genes, characterized by enhanced fitness of a double mutant suggest that these genes are likely to associate physically or act in the same pathway.

The fitness of the double mutants was analyzed at elevated temperatures and in the presence of cantharidin. Both *cacrg1*Δ/Δ*sld1*Δ/Δ and *cacrg1*Δ/Δ*mts1*Δ/Δ double mutants showed drastically altered fitness in liquid medium at 39 °C compared

dx.doi.org/10.1021/cb400607h | *ACS Chem. Biol.* 2013, 8, 2785−2793

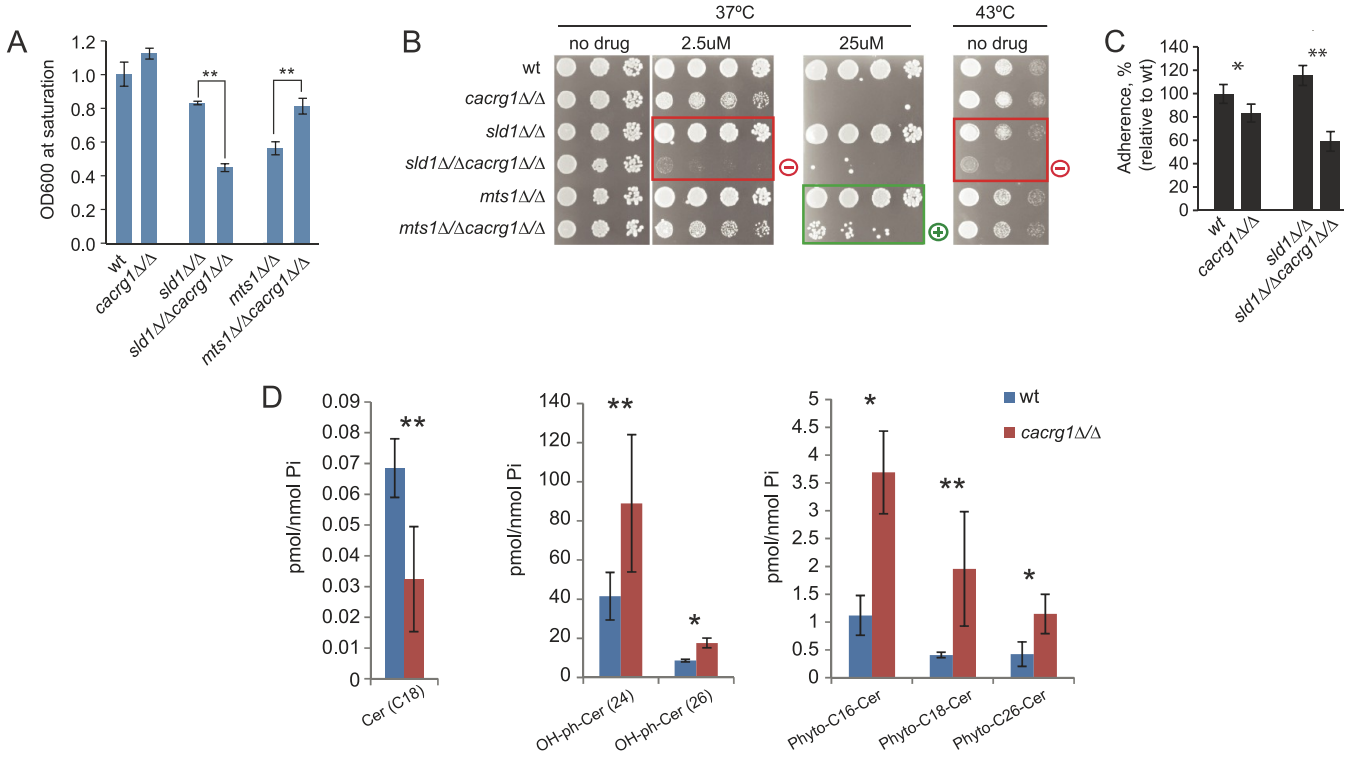

Figure 6. CaCrg1 is important for sphingolipid biosynthesis. (A) Fitness of double deletion mutants in liquid SC media at 39 °C. (B) *CaCRG1* interacts with GlcCer genes in a condition-dependent manner. The unexpected phenotypes for double mutants (relative to wt and *crg1*Δ/Δ mutant) are highlighted: "+" denotes positive genetic interactions, "−" denotes negative genetic interaction. (C) Adherence of *cacrg1*Δ/Δ*sld1*Δ/Δ to abiotic surface. (D) Abundance of ceramide-related species in *cacrg1*Δ/Δ and wt. Statistically significant difference in the abundance (Student's *t* test) is shown in red. Error bars are standard deviation. *P-value < 0.05, **P-value < 0.1, Student's *t* test.

to the single mutants and wt (Figure 6A). Specifically, the double homozygous deletion strain *cacrg1*Δ/Δ*sld1*Δ/Δ is synthetically sick (negative genetic interaction) at 39 °C in liquid media and at 43 °C on solid SD media. *cacrg1*Δ/Δ*mts1*Δ/Δ mutant showed alleviating (positive) interactions at 39 °C and in the presence of cantharidin (Figure 6A and B). Because neither of these genes were sensitive as single mutants, the effect is specific to the double mutant combination. *CaCRG1* also had a negative genetic interaction with *HSX11* and *HET1* in the presence of cantharidin (50 μM) at 30 °C (Supplementary Figure 6A). Additionally, we observed synthetic lethality in a *cacrg1*Δ/Δ*sld1*Δ/Δ mutant grown at 37 °C and cantharidin (2.5 μM) and an enhanced fitness of *cacrg1*Δ/Δ*mts1*Δ/Δ mutant at 37 °C and cantharidin (25 μM). The genetic interactions between CaCrg1 and sphingolipid-modifying enzymes in the presence of the compound may reflect a critical role of sphingolipids in sustaining the barrier function of the plasma membrane toward compounds such as cantharidin.

Phenotypically, *cacrg1*Δ/Δ*sld1*Δ/Δ had significantly reduced adherence to plastic (Figure 6C) and had a drastically different morphological appearance compared to wt and the corresponding single deletion mutants (Supplementary Figure 6B). The observation of negative and positive genetic interactions between *CaCRG1* and GlcCer genes (*e.g.*, sphingolipid delta-8 desaturase *SLD1*) based on fitness and other phenotypes, such as adhesion and colony morphology, suggests that *CaCRG1* is required to buffer the absence of these genes in stress. Thus, *CaCRG1* may act in a parallel pathway to the GlcCer pathway. The positive or suppressive interaction observed between *CaCRG1* and *MTS1* indicates that the product of Mts1 may be toxic in the absence of CaCrg1 (*e.g.*, membrane integrity is compromised), and therefore the absence of both *MTS1* and *CaCRG1* results in an increased fitness of a mutant.

Deletion of *CaCRG1* Results in the Accumulation of Phytoceramides. To further investigate the effect of deletion of *CaCRG1* on the levels of sphingolipids, we measured the abundance of ceramides, GlcCer, and precursors for inositol-containing sphingolipids in wt and *cacrg1* deletion mutants. Deletion of *CaCRG1* resulted in a significant increase in OH-ceramides and phytoceramides compared to the levels in wt (Figure 6D): OH-phytoCer (26) (P-value < 0.04), OH-phytoCer (24) (P-value < 0.1), phyto-C16-Cer (P-value < 0.05), phyto-C18-Cer (P-value < 0.06), and phyto-C26-Cer (P-value < 0.04). This accumulation of specific precursors of inositol-containing sphingolipid species in the mutant indicates that CaCrg1 functions in this branch of the complex sphingolipid pathway for the generation of GlcCer. Furthermore, these results are consistent with our genetic interaction analysis, which demonstrated that *CaCRG1* may act in either parallel or overlapping pathways with GlcCer biosynthesis. For example, CaCrg1 may play a role either in a conversion of phytoceramides to complex inositol-containing sphingolipids (IPC and MIPC) by methylating specific phytoceramides or in a negative regulation of the breakdown of the complex inositol-containing sphingolipids (*via* a salvage pathway). Combined, these data show that CaCrg1, along with these other gene products, is important in complex sphingolipid biosynthesis *in vivo*. The mechanistic relationships between these pathway components will require detailed follow-up studies.

CaCrg1 Is Important for *C. albicans* Virulence in *Galleria mellonella*. Sphingolipid biosynthesis has been

dx.doi.org/10.1021/cb400607h | *ACS Chem. Biol.* 2013, 8, 2785−2793

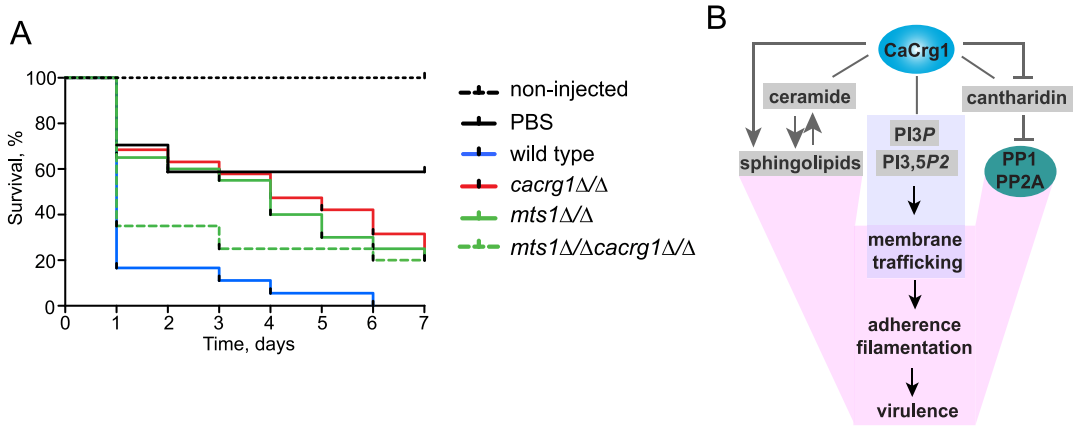

Figure 7. CaCrg1 is important for *C. albicans* virulence in *Galleria mellonella*. (A) Kaplan–Meier survival plot demonstrating that the deletion of *CaCRG1* results in increased survival (relative to wt) of *G. mellonella larvae* injected with *C. albicans*. (B) A model demonstrating how CaCrg1 and it functional interactions play a role in drug response and fungal virulence. CaCrg1 interacts with toxic cantharidin that inhibits protein phosphatases involved in multiple biological processes. Upon the drug exposure *CaCRG1* maintains membrane trafficking, adhesion and hyphal elongation, the processes required for fungal virulence.

implicated in the virulence of pathogenic fungi.[25−28] Therefore, to test the role of CaCrg1 in the pathogenicity of *C. albicans*, we examined the effect of deletion of *CaCRG1* on infectivity of the greater wax moth *G. mellonella*, an established invertebrate model of infection.[31,32] At least 16 larvae were used for each treatment and controls using a single blind design. Each larvae was injected with 5×10^5 stationary phase cells, incubated at 37 °C and assessed for viability every 24 h. We found that *mts*Δ/Δ has decreased virulence in the infected waxmoth larvae (Figure 7A), in accordance with the previous infection experiments performed in mice.[28] A survival analysis of the infected larvae revealed that the deletion of *CaCRG1* also significantly attenuated the virulence *of C. albicans* compared to wt injected larvae (*P*-value < 0.0001, log-rank test). We also found that *cacrg1*Δ/Δ*mts1*Δ/Δ has increased virulence relative to the single mutants, suggesting that the condition-dependent positive genetic interactions we observed between *CaCRG1* and *MTS1 in vitro* can be recapitulated in the infection model. Our findings demonstrate that CaCrg1 plays a role in host–pathogen interactions. One plausible explanation of these observations is that CaCrg1 is important for fungal virulence *via* the regulation of the levels of phytoceramides, yet further evidence is required to support this conclusion. Furthermore, as-yet-unidentified endogenous substrates of CaCrg1 are likely involved in pathogenesis and may be revealed under these conditions.

In summary, we demonstrated that *C. albicans* CaCrg1 is a *bona fide* smMTase that interacts with the cytotoxic cantharidin *in vitro* and *in vivo* and other lipid molecules contributing to its biological role (Figure 7B). We found that CaCrg1 is important for virulence-related processes such as adhesion, hyphal elongation, and membrane trafficking in the response to cantharidin. CaCrg1 is related to complex sphingolipid biosynthesis: it binds to exogenous short-chain ceramides *in vitro*, it interacts genetically with genes of the GlcCer pathway, and the deletion of *CaCRG1* leads to significant changes in the abundance of OH-ceramides and phytoceramides required for the biosynthesis of complex sphingolipids. Finally we found that this novel lipid-related smMTase is required for virulence in the waxmoth *Galleria mellonella*, a model of infection.

METHODS

Strains and Growth Conditions. Yeast strains and plasmids are described in Supplementary Table 3 and 4, respectively. Cantharidin (Sigma Aldrich) was dissolved in DMSO and stored at −20 °C. Ceramides (*N*-acetylshphingosine, *N*-octanoylsphingosine, *N*-palmitoylsphingosine) were from Avanti Polar Lipids, Inc., dissolved in DMSO or ethanol. Cells analyzed by spot dilutions were normalized to an equal OD_{600}, 10-fold diluted, spotted onto solid media, and incubated at 30 °C for 2 days.

Microarray Analysis. Cells grown to mid-exponential phase in YPD were incubated with cantharidin (2 mM) for 30 min and harvested by centrifugation. Isolation of RNA and hybridization to the microarrays was performed as described.[11] Three independent replicates were used for the analyses. Hybridization to Affymetrix custom expression array (stCANDIDA 1a) (Affymetrix) was followed by the extraction of intensity values for the probes using the GeneChip Operating Software (Affymetrix). The resulting files containing probe position and intensities were analyzed by aligning the probes that match the position of the *Candida* Genome Database list of defined ORFs. Quantile normalized data sets were further analyzed (Supplementary Table 1). The significance for a differential expression was set as $\log_2$ (drug/DMSO) > |2|, *P*-value < 0.05 as determined by Student's *t* test. Significantly up- and downregulated transcripts were further tested for Gene Ontology (GO) Biological process term enrichment using AmiGo (http://amigo.geneontology.org) with *P*-value cutoff of 0.05 and multiple testing corrections (Bonferroni).

Cloning and Purification of CaCrg1 Fusion Protein. The sequence of *CaCRG1* was optimized for expression in *S. cerevisiae* and synthesized with sequences for restriction enzyme digestion sites BsrGI in the universal vector pUC57. The synthesized *CaCRG1* was cut out with BsrGI, SAP-treated, and co-transformed with BsrGI-linearized BG1805 vector into a *S. cerevisiae crg1*Δ/Δ mutant. *CaCRG1* was cloned downstream of a *GAL1* inducible promoter and in frame with a triple affinity tag at C-terminal (His_6-$HA^{epitope}$-$3C^{protease\ site}$-$ZZ^{protein\ A}$). Transformants were screened by PCR and for cantharidin resistance. Clones were sequence-verified. To express CaCrg1, cells were grown to mid-exponential phase in SD-Ura containing 2% raffinose and then induced with 2% galactose. Cells were harvested after overnight induction, and CaCrg1 expression was verified by *anti*-HA antibodies. Induction and purification of CaCrg1 was performed as described previously.[11]

Site-Directed Mutagenesis. *CaCRG1* missense and deletion mutants were prepared using the Phusion Site-directed mutagenesis kit (Thermo Fisher) with the primers listed in Supplementary Table 5. Clones were sequence-verified. To express mutated CaCrg1, transformants were grown to mid-exponential phase in SD-Ura and 2%

dx.doi.org/10.1021/cb400607h | *ACS Chem. Biol.* 2013, 8, 2785−2793

raffinose and induced by the addition of 2% galactose. Cantharidin (30 μM) was used to test the sensitivity of mutants. Cells were harvested after 3 h of induction, and CaCrg1 expression was verified with *anti*-HA antibodies.

Metabolomic Profiling of *C. albicans* Cellular Extracts. Wt and *cacrg*Δ/Δ mutants were cultured in the presence of cantharidin, and cellular extracts were prepared for metabolomic analysis by mass spectrometry based on methods described previously.[11] Briefly, cells were cultured in SC medium overnight at 30 °C. Mid-exponential cells were treated with cantharidin (100 μM) or DMSO alone (1%). After 90 min of growth at 30 °C, cells were rapidly isolated onto 45-mm diameter Millipore nylon filter membranes (0.45-μm pore size) *via* vacuum filtration. The filter was then transferred to a Petri dish containing 800 μL of 80:20 acetonitrile/H_2O, and the dish was incubated at 4 °C for 15 min before the extract was transferred to a tube. The filters were washed again with 200 μL of extraction buffer. The extract was centrifuged at 20,800 rcf for 5 min, and the supernatant was isolated. The pellet was re-extracted with 200 μL of extraction buffer and incubated at 4 °C for 15 min. After centrifugation at 20,800 rcf for 5 min, the supernatants from both extraction steps were pooled, neutralized with 120 μL of 15% ammonium bicarbonate, dried by vacuum centrifugation, and frozen. The samples were resuspended in 100 μL of H_2O before analysis by LC−MS/MS using methods that we described previously.[11]

***In Vitro* Methylation Reactions.** Reaction mixtures containing 0.2 mM cantharidin (prepared as a stock solution of 10 mM cantharidin in DMSO) and 20 μM *S*-adenosyl-[methyl-^{14}C]-L-methionine (48.8 mCi/mmol; PerkinElmer Inc.) in a buffer of 0.1 M sodium phosphate, pH 7.4, were mixed with either 0.015 μg, 0.03 μg, or 0.06 μg of recombinant *C. albicans* CaCrg1 protein in a final volume of 50 μL. Control reactions were performed in the absence of protein (no enzyme) or in the absence of cantharidin (DMSO solvent alone) with 0.09 μg of the CaCrg1 protein. Samples were incubated for 120 min at 30 °C, and the reaction was quenched by the addition of 40 μL of 2 M HCl. Methylation of cantharidin was determined by acid-labile volatility as described previously.[11] A portion of the quenched reaction mixture (80 μL) was spotted on a filter paper, which was then placed in a scintillation vial containing 5 mL of Safety-Solve cocktail (Research Products International) and incubated for 4 h at RT. Radioactivity released as ^{14}C-methanol was measured by counting the vial after removal of the paper.

Lipid−Protein Overlay Assay. The Screen-Well Bioactive lipid library containing 195 bioactive lipids (Supplementary Table 2) from Enzo Life Sciences, Inc. was spotted onto FAST glass slides covered with nitrocellulose polymer (Whatman Ltd., GE Healthcare), and the binding between CaCrg1 and lipids was analyzed by standard lipid-overlay assay. Briefly, lipids dissolved in chloroform/methanol/water (1:2:0.8) were spotted on PVDF membrane. Dried membranes were blocked for 1 h in 3% fatty acid-free BSA in TBST (50 mM Tris/HCl pH 7.5, 150 mM NaCl, 0.1% Tween20). The arrays were incubated with affinity purified HA-tagged CaCrg1 (2 μg mL^{-1}) overnight at 4 °C with gentle stirring. The membrane was washed six times for 30 min in TBST, incubated with mouse anti-HA monoclonal antibody for 1 h, washed again as before, incubated with anti-mouse-horseradish peroxidase conjugate. Finally, the membrane was washed 12 times for 1 h in TBST, and the membrane-bound HA-fusion CaCrg1 was detected by ECL.

FM4-64 Labeling for Vacuolar Membrane Dynamics. Wt and *cacrg1*Δ/Δ cells were grown overnight in SC. Cells grown to mid-exponential phase in YPD a 30 °C were concentrated to OD_{600} of 20, and stained with lipophilic dye FM4-64 (40 μM) for 45 min at 25 °C. Cells were washed twice and resuspended in 200 μL of YPD. Cells were treated with 250 μM cantharidin and incubated at 30 °C for 1 h with shaking. Cells were observed after 15 min and 1 h of cantharidin treatment with 63x objective, and fluorescence images (Cy3 filter) were acquired using AxioVision software on an Axiovert 200 M fluorescence microscope (Zeiss).

***C. albicans* Adhesion Assay.** Wt and *cacrg11*Δ/Δ cells grown in YPD at 30 °C overnight were washed twice with PBS pH 7.4. Cells were inoculated into SC media to final OD_{600} of 0.5. After 2 h at 37 °C, nonadherent cells were removed by three PBS washes. Adherent cells were stained with 0.1% crystal violet for 5 min and then washed with PBS three times, 0.25% SDS once, and with PBS twice. Crystal violet was solubilized with 150 μL isopropyl alcohol/0.04 N HCl and 50 μL of 0.25% SDS. The absorbance of each well was measured as A_{590}.

Quantitative Real-Time PCR Analysis. Cells grown to mid-exponential phase in YPD medium were incubated with cantharidin for varying amounts of time, harvested by centrifugation, frozen in liquid N_2 and stored at −80 °C. RNA extraction and QRT-PCR analysis was performed as described.[11]

Construction of Double Mutants. Double knockout strains were generated using *SAT* technology.[33] *SAT* was PCR amplified from pJK863 (pLC49) using specific primers (Supplementary Table 5), containing sequence homologous to *SAT* and a gene of interest. PCR-amplified product was transformed into strains using standard transformation protocol. Nourseothricin (NAT)-resistant transformants were PCR tested for proper integration of the construct. The *SAP2* promoter was induced to drive expression of FLP recombinase to excise the NAT marker cassette for a subsequent reuse. The procedure was repeated until all alleles were knocked out with *SAT* cassette. This strain was additionally tested for the absence of any wt alleles by PCR.

Mass Spectrometry Analysis of Lipids. Total lipids were extracted as described.[34] Briefly, wt and *cacrg1* null mutants were grown at 39 °C for 48 h in SC media. Cells were washed twice with PBS and counted. Cells (5×10^8) were placed in a single glass tube, and lipids were extracted using Mandala followed by Bligh and Dyer extraction. A quarter of the lipid samples were used for inorganic phosphate determination. The remaining lipids were analyzed by MS and MS/MS scans using a TSQ7000 triple quadruple mass spectrometer with electrospray ionization as described.

Virulence Assay. The *C. albicans* virulence assay was performed on waxworm larvae of *G. mellonella*. Larvae were obtained from Port Credit Pet Center, Ontario. *C. albicans* cells grown overnight in YPD at 30 °C were washed with PBS, and 5×10^5 cells were injected into the larvae in 20 μL of PBS and incubated at 37 °C. Dead larvae were scored daily. Kaplan−Meier plots were generated using GraphPad Prism software, and significant difference in survival was analyzed by log-rank test.

■ ASSOCIATED CONTENT

Ⓢ Supporting Information

This material is available free of charge *via* the Internet at http://pubs.acs.org.

■ AUTHOR INFORMATION

Corresponding Author

*E-mail: corey.nislow@ubc.ca.

Notes

The authors declare no competing financial interest.

■ ACKNOWLEDGMENTS

We thank M. Gebbia, T. Durbic, and A. Surendra for experimental assistance and L. Cowen for providing the plasmids. We also thank P. Yau for assistance with printing lipids onto FAST slides. E.L. was supported by Ontario Graduate Scholarship and University of Toronto Open Fellowship. C.N. and G.G. are supported by grants from the NHGRI and the Canadian Cancer Society (Grant 020380), and S.G.C. is supported by NIH grant GM026020. The funders had no role in study design, data collection and analysis, decision to publish, or preparation of the manuscript.

REFERENCES

(1) Peleg, A. Y., Hogan, D. A., and Mylonakis, E. (2010) Medically important bacterial-fungal interactions. *Nat. Rev. Microbiol. 8*, 340−349.

(2) Odds, F. C. (1987) Candida infections: an overview. *Crit. Rev. Microbiol. 15*, 1−5.

(3) Petrossian, T. C., and Clarke, S. G. (2009) Multiple Motif Scanning to identify methyltransferases from the yeast proteome. *Mol. Cell. Proteomics 8*, 1516−1526.

(4) Bentley, R., and Chasteen, T. G. (2002) Microbial methylation of metalloids: arsenic, antimony, and bismuth. *Microbiol. Mol. Biol. Rev. 66*, 250−271.

(5) Bach, S. J. (1945) Biological methylation. *Biol. Rev. Cambridge Philos. Soc. 20*, 158−176.

(6) Fujioka, M. (1992) Mammalian small molecule methyltransferases: their structural and functional features. *Int. J. Biochem. 24*, 1917−1924.

(7) Wlodarski, T., Kutner, J., Towpik, J., Knizewski, L., Rychlewski, L., Kudlicki, A., Rowicka, M., Dziembowski, A., and Ginalski, K. (2011) Comprehensive structural and substrate specificity classification of the Saccharomyces cerevisiae methyltransferome. *PLoS One 6*, e23168.

(8) Luo, M. (2012) Current chemical biology approaches to interrogate protein methyltransferases. *ACS Chem. Biol. 7*, 443−463.

(9) Petrossian, T., and Clarke, S. (2009) Bioinformatic identification of novel methyltransferases. *Epigenomics 1*, 163−175.

(10) Hoon, S., Smith, A. M., Wallace, I. M., Suresh, S., Miranda, M., Fung, E., Proctor, M., Shokat, K. M., Zhang, C., Davis, R. W., Giaever, G., St, Onge, R. P., and Nislow, C. (2008) An integrated platform of genomic assays reveals small-molecule bioactivities. *Nat. Chem. Biol. 4*, 498−506.

(11) Lissina, E., Young, B., Urbanus, M. L., Guan, X. L., Lowenson, J., Hoon, S., Baryshnikova, A., Riezman, I., Michaut, M., Riezman, H., Cowen, L. E., Wenk, M. R., Clarke, S. G., Giaever, G., and Nislow, C. (2011) A systems biology approach reveals the role of a novel methyltransferase in response to chemical stress and lipid homeostasis. *PLoS Genet. 7*, e1002332.

(12) Eisner, T., Smedley, S. R., Young, D. K., Eisner, M., Roach, B., and Meinwald, J. (1996) Chemical basis of courtship in a beetle (Neopyrochroa flabellata): Cantharidin as "nuptial gift". *Proc. Natl. Acad. Sci. U.S.A. 93*, 6499−6503.

(13) Eisner, T., Smedley, S. R., Young, D. K., Eisner, M., Roach, B., and Meinwald, J. (1996) Chemical basis of courtship in a beetle (Neopyrochroa flabellata): cantharidin as precopulatory "enticing" agent. *Proc. Natl. Acad. Sci. U.S.A. 93*, 6494−6498.

(14) Laidley, C. W., Cohen, E., and Casida, J. E. (1997) Protein phosphatase in neuroblastoma cells: [3H]cantharidin binding site in relation to cytotoxicity. *J. Pharmacol. Exp. Ther. 280*, 1152−1158.

(15) Efferth, T., Rauh, R., Kahl, S., Tomicic, M., Bochzelt, H., Tome, M. E., Briehl, M. M., Bauer, R., and Kaina, B. (2005) Molecular modes of action of cantharidin in tumor cells. *Biochem. Pharmacol. 69*, 811−818.

(16) Li, Y. M., and Casida, J. E. (1992) Cantharidin-binding protein: identification as protein phosphatase 2A. *Proc. Natl. Acad. Sci. U.S.A. 89*, 11867−11870.

(17) Honkanen, R. E. (1993) Cantharidin, another natural toxin that inhibits the activity of serine/threonine protein phosphatases types 1 and 2A. *FEBS Lett. 330*, 283−286.

(18) Pfaller, M. A., and Diekema, D. J. (2007) Epidemiology of invasive candidiasis: a persistent public health problem. *Clin. Microbiol. Rev. 20*, 133−163.

(19) Korting, H. C., Schlaf-Maier, U., and Schafer-Korting, M. (1986) [Antimicrobial effects of in vitro-simulated ketoconazole-cantharidin blister fluid levels on candida albicans]. *Mykosen 29*, 297−305.

(20) Zakikhany, K., Thewes, S., Wilson, D., Martin, R., Albrecht, A., and Hube, B. (2008) From attachment to invasion: infection associated genes of Candida albicans. *Nihon Ishinkin Gakkai Zasshi 49*, 245−251.

(21) Vida, T. A., and Emr, S. D. (1995) A new vital stain for visualizing vacuolar membrane dynamics and endocytosis in yeast. *J. Cell Biol. 128*, 779−792.

(22) Michell, R. H., Heath, V. L., Lemmon, M. A., and Dove, S. K. (2006) Phosphatidylinositol 3,5-bisphosphate: metabolism and cellular functions. *Trends Biochem. Sci. 31*, 52−63.

(23) Gillooly, D. J., Raiborg, C., and Stenmark, H. (2003) Phosphatidylinositol 3-phosphate is found in microdomains of early endosomes. *Histochem. Cell Biol. 120*, 445−453.

(24) Hannun, Y. A., and Obeid, L. M. (2008) Principles of bioactive lipid signalling: lessons from sphingolipids. *Nat. Rev. Mol. Cell Biol. 9*, 139−150.

(25) Heung, L. J., Luberto, C., and Del Poeta, M. (2006) Role of sphingolipids in microbial pathogenesis. *Infect. Immun. 74*, 28−39.

(26) Ramamoorthy, V., Cahoon, E. B., Thokala, M., Kaur, J., Li, J., and Shah, D. M. (2009) Sphingolipid C-9 methyltransferases are important for growth and virulence but not for sensitivity to antifungal plant defensins in Fusarium graminearum. *Eukaryotic Cell 8*, 217−229.

(27) Oura, T., and Kajiwara, S. (2010) Candida albicans sphingolipid C9-methyltransferase is involved in hyphal elongation. *Microbiology 156*, 1234−1243.

(28) Noble, S. M., French, S., Kohn, L. A., Chen, V., and Johnson, A. D. (2010) Systematic screens of a Candida albicans homozygous deletion library decouple morphogenetic switching and pathogenicity. *Nat. Genet. 42*, 590−598.

(29) Ternes, P., Sperling, P., Albrecht, S., Franke, S., Cregg, J. M., Warnecke, D., and Heinz, E. (2006) Identification of fungal sphingolipid C9-methyltransferases by phylogenetic profiling. *J. Biol. Chem. 281*, 5582−5592.

(30) Tong, A. H., Lesage, G., Bader, G. D., Ding, H., Xu, H., Xin, X., Young, J., Berriz, G. F., Brost, R. L., Chang, M., Chen, Y., Cheng, X., Chua, G., Friesen, H., Goldberg, D. S., Haynes, J., Humphries, C., He, G., Hussein, S., Ke, L., Krogan, N., Li, Z., Levinson, J. N., Lu, H., Menard, P., Munyana, C., Parsons, A. B., Ryan, O., Tonikian, R., Roberts, T., Sdicu, A. M., Shapiro, J., Sheikh, B., Suter, B., Wong, S. L., Zhang, L. V., Zhu, H., Burd, C. G., Munro, S., Sander, C., Rine, J., Greenblatt, J., Peter, M., Bretscher, A., Bell, G., Roth, F. P., Brown, G. W., Andrews, B., Bussey, H., and Boone, C. (2004) Global mapping of the yeast genetic interaction network. *Science 303*, 808−813.

(31) Fallon, J., Kelly, J., and Kavanagh, K. (2012) Galleria mellonella as a model for fungal pathogenicity testing. *Methods Mol. Biol. 845*, 469−485.

(32) Brennan, M., Thomas, D. Y., Whiteway, M., and Kavanagh, K. (2002) Correlation between virulence of Candida albicans mutants in mice and Galleria mellonella larvae. *FEMS Immunol. Med. Microbiol. 34*, 153−157.

(33) Reuss, O., Vik, A., Kolter, R., and Morschhauser, J. (2004) The SAT1 flipper, an optimized tool for gene disruption in Candida albicans. *Gene 341*, 119−127.

(34) Singh, A., Qureshi, A., and Del Poeta, M. (2011) Quantitation of cellular components in Cryptococcus neoformans for system biology analysis. *Methods Mol. Biol. 734*, 317−333.

SUPPORTING INFORMATION

A Novel Small Molecule Methyltransferase is Important for Virulence in *Candida albicans*

Elena Lissina[1], David Weiss[2], Brian Young[2], Antonella Rella[3], Kahlin Cheung-Ong[1], Maurizio Del Poeta[3], Steven G. Clarke[2], Guri Giaever[4], and Corey Nislow[4*]

Supplementary Figure Legends:

Supplementary Figure 1

A. Diagram of cloning and subcloning steps of the synthesized *CaCRG1* onto BG1805 vector.
B. Analysis of the levels of wt and mutated CaCrg1 proteins by immunoblotting. Cells were grown overnight in SD-ura, diluted to OD_{600} of 0.2 and grown to mid-exponential stage (OD_{600} of 0.8). The expression was induced in YP and galactose (2%) for 3 hours. The cell lysates were analyzed by anti-HA antibody.

Supplementary Figure 2

Possible effectors of CaCrg1 enzyme activity show little effect on methylation of cantharidin. Addition of 1 mM DTT, 2 mM EGTA, 0.5 mM imidazole, or 0.2 mM sodium chloride to reactions with 0.0225 µg of CaCrg1 enzyme do not significantly alter enzyme activity as measured by acid-labile methylation assays. Error bars represent standard deviation from duplicate samples in one single experiment.

Supplementary Figure 3

CaCRG1 is required for adhesion of cells to plastic surface at log phase at 37ºC. Wt and *cacrg1Δ/Δ* mutants were grown overnight in liquid YPD, diluted to OD_{600} of 0.2 and grown to mid-exponential stage (OD_{600} of 0.8) in SC media. Cells were diluted to 0.5 OD_{600} in SC media and incubated at 30ºC or 37ºC for 2hrs. * *p*-value <0.01.

Supplementary Figure 4

A. Simplified diagram of endocytic pathway. CaCrg1 interacts with phosphoinositides PI(3)*P* and PI(3,5)*P2* known to be associated with the membranes of early and later endosomes.
B. Fluorescence imaging of co-localization of GFP-tagged ScCrg1 and vacuolar membrane stain FM4-64 in the baker's yeast after overnight treatment with cantharidin (50 μM). .

Supplementary Figure 5

A. C16-ceramide - CaCrg1 overlay assay. Biologically active C16-ceramide was spotted onto nitrocellulose membrane. Affinity purified CaCrg1 (19 pmol; 1 ug/ml) was incubated with C16-ceramide overnight at 4ºC and its binding was assessed with anti-HA antibody. Quantification of relative binding of CaCrg1 to ceramide was performed with ImageJ software.
B. Sphingolipid-protein overlay assay of CaCrg1. 6xHis tagged CaCrg1 was expressed in baker's yeast followed by affinity purification. CaCrg1 (38 pmol; 2ug/ml) was incubated with lipid-spotted membrane overnight at 4ºC. After rigorous washing, the binding of CaCrg1 to sphingolipids (100 pmol per spot) was detected using anti-HA antibody.

Supplementary Figure 6

A. *CaCRG1* interacts with GlcCer-related genes in a condition-dependent manner. Overnight cultures were 10-fold diluted, spotted onto SC defined medium with or without cantharidin and incubated at various temperatures (37 ºC and 43 ºC). The unexpected phenotypes for double deletion mutants (relative to wt and *crg1*Δ/Δ mutant) are highlighted: "+" denotes positive genetic interactions, "-" denotes negative genetic interaction.
B. Morphology of *C. albicans* wt and mutant cells. Cells were streaked onto solid YPD media and incubated at 37 °C for 5 days. Bar, 2mm.

Supplementary Table 1. Differentially expressed genes in *C. albicans* wt cells treated with cantharidin (2 mM, 30 min).

Supplementary Table 2. Bioactive lipids present on the array.

Supplementary Table 3. Yeast strains used in this study.

Supplementary Table 4. Plasmids used in this study.

Supplementary Table 5. Primers used in this study.

Supplementary Table 1. Differentially expressed genes in *C. albicans* wt cells treated with cantharidin (2 mM, 30 min).

ORF	*GENE*	Mean DMSO	Mean drug	Log2 (drug/DMSO)	T-test, *p*-val (2,2)
orf19.6475		53.03	9379.51	7.5	0.00010
orf19.1048	*IFD6*	18.93	3283.63	7.4	0.00571
orf6.2005		2.54	316.44	7.0	0.00875
orf19.4173	*ScDPH2*	55.97	6731.72	6.9	0.00434
orf19.2713	*ScMSH5*	8.39	868.15	6.7	0.00355
orf19.5604	*MDR1*	16.94	1338.45	6.3	0.00347
orf19.629	*IFD7*	6.67	425.83	6.0	0.00150
orf19.3848		53.61	1814.50	5.1	0.00922
orf19.4309	*GRP2*	44.31	993.20	4.5	0.00012
orf19.7296		29.42	618.37	4.4	0.00319
orf6.4916		12.31	210.82	4.1	0.00016
orf19.2451	*PGA45*	32.88	533.30	4.0	0.00431
orf19.3735		18.27	228.68	3.6	0.00100
orf19.4477	*CSH1*	33.28	369.28	3.5	0.00157
orf19.2023	*HGT7*	133.77	1039.73	3.0	0.02302
orf19.7085		78.12	525.47	2.7	0.01160
orf19.633	*CaCRG1*	200.37	986.84	2.3	0.00090
orf19.251	*ScHSP31*	119.47	544.13	2.2	0.00274
orf19.5806	*ALD5*	609.95	2671.22	2.1	0.00336
orf19.4631	*ERG251*	327.36	1410.31	2.1	0.00686
orf19.1426		534.51	137.64	-2.0	1.9E-04
orf19.7492	*SWC4*	233.12	59.97	-2.0	2.6E-05
orf19.5599	*MDL2*	243.86	62.69	-2.0	9.1E-04
orf19.1607	*ALR1*	374.28	96.22	-2.0	4.8E-03
orf6.1737		773.62	198.45	-2.0	6.7E-03
orf19.1490	*MSB2*	310.23	79.38	-2.0	3.3E-03
orf19.6114		1517.96	387.56	-2.0	8.5E-03
orf19.1623	*CAP1*	247.04	62.60	-2.0	2.4E-03
orf19.866	*RAD32*	312.07	78.96	-2.0	5.5E-04
orf19.3752	*RAD51*	360.51	91.11	-2.0	1.4E-02
orf19.5676		210.81	53.23	-2.0	1.5E-03
orf19.5148	*CYR1*	284.23	71.69	-2.0	6.6E-03
orf19.6476	*ScAVL9*	245.29	61.80	-2.0	6.8E-04
orf19.789	*PYC2*	241.54	60.77	-2.0	2.5E-02
orf19.5908	*TEC1*	486.13	122.17	-2.0	4.5E-03

orf19.3858		224.49	56.14	-2.0	3.8E-06
orf19.2990	*XOG1*	231.64	57.89	-2.0	7.6E-03
orf6.2673		2955.41	735.23	-2.0	8.7E-05
orf19.4772	*SSU81*	402.77	100.17	-2.0	3.7E-04
orf19.7123		481.84	119.78	-2.0	5.3E-03
orf19.6745	*TPI1*	3343.17	830.10	-2.0	1.5E-03
orf19.3926		266.56	66.17	-2.0	2.4E-03
orf19.1806		214.78	53.30	-2.0	2.6E-03
orf19.1658		549.76	136.27	-2.0	2.2E-03
orf19.1135	*CAS1*	452.47	111.72	-2.0	8.5E-04
orf19.3630	*RRP8*	863.37	212.94	-2.0	6.6E-05
orf19.2051	*ScRPN4*	336.69	83.02	-2.0	5.9E-03
orf19.4281		310.53	76.38	-2.0	2.3E-04
orf19.3644		978.79	240.18	-2.0	8.1E-05
orf19.6121	*MNL1*	214.67	52.14	-2.0	4.5E-03
orf19.6493		559.48	135.80	-2.0	9.7E-04
orf19.4820		224.86	54.10	-2.1	4.9E-04
orf19.6573	*BEM2*	883.57	212.34	-2.1	1.7E-03
orf19.723	*BCR1*	358.56	85.78	-2.1	3.0E-03
orf19.5071	*NRP1*	450.09	106.93	-2.1	4.9E-05
orf19.6202	*RBT4*	394.16	93.41	-2.1	3.8E-03
orf19.4346		933.18	220.99	-2.1	4.8E-03
orf19.1685		253.81	59.98	-2.1	1.3E-02
orf19.7278		1644.19	387.85	-2.1	3.9E-02
orf19.5041		300.70	70.82	-2.1	2.7E-04
orf19.4728	*ScHOS4*	294.68	69.33	-2.1	9.5E-04
orf19.7079		208.27	48.97	-2.1	1.1E-03
orf6.326		498.90	117.17	-2.1	1.5E-04
orf19.5678	*ScDPH2*	296.46	69.58	-2.1	7.9E-04
orf19.1842		352.63	82.70	-2.1	1.2E-04
orf19.4775	*CTA8*	639.66	149.36	-2.1	9.8E-06
orf19.7150	*NRG1*	829.72	193.69	-2.1	3.1E-03
orf19.2460		231.70	53.87	-2.1	1.3E-02
orf19.6186		252.94	58.57	-2.1	3.7E-03
orf19.6713		424.30	98.23	-2.1	6.9E-05
orf19.1281		208.12	48.00	-2.1	1.3E-04
orf19.3252		219.57	50.21	-2.1	1.8E-05
orf19.4377	*KRE1*	702.67	160.37	-2.1	7.7E-04
orf19.182		1709.35	389.72	-2.1	5.8E-03
orf19.2331	*ADA2*	205.35	46.78	-2.1	3.3E-03
orf19.2877	*PDC11*	7456.90	1691.80	-2.1	9.4E-03
orf19.5903	*RAX1*	273.83	61.83	-2.1	2.9E-03
orf6.895		373.42	83.86	-2.2	6.1E-05
orf19.2812		1543.60	346.39	-2.2	7.2E-03
orf19.932		510.83	114.09	-2.2	3.9E-04
orf19.3678		281.27	62.73	-2.2	2.9E-03
orf19.1741		4474.98	996.82	-2.2	2.0E-03
orf19.5469	*HPR5*	447.01	99.42	-2.2	2.8E-02
orf19.3728	*ScGIP4*	246.09	54.60	-2.2	2.5E-03
trna6.2289.1.5prime		201.30	44.44	-2.2	7.9E-05
orf19.5483		224.08	49.33	-2.2	7.5E-05
orf6.579		684.20	150.59	-2.2	3.9E-04
orf19.4225	*LEU3*	263.29	57.84	-2.2	1.8E-04
orf19.2501	*FLC1*	350.16	76.46	-2.2	3.7E-02
orf19.1871	*ScSWR1*	432.63	94.24	-2.2	1.6E-06
orf6.3074		938.23	204.29	-2.2	2.8E-03

orf19.1277		486.81	105.82	-2.2	3.7E-03
orf6.2111		203.57	43.93	-2.2	2.3E-03
orf19.4555	*ALS4;*	133.41	28.70	-2.2	2.4E-03
orf19.3083		337.63	72.50	-2.2	6.7E-03
orf19.1103		324.62	69.61	-2.2	9.4E-04
orf19.1393		216.91	46.48	-2.2	2.3E-03
orf19.2296		503.18	107.47	-2.2	6.8E-03
orf19.7506		210.82	45.02	-2.2	2.9E-03
orf19.469	*HST7*	369.95	78.94	-2.2	9.9E-04
orf19.1259		224.63	47.75	-2.2	6.4E-05
orf19.4099	*ECM17*	358.01	75.87	-2.2	7.1E-06
orf19.6760	*MDS3*	279.29	59.16	-2.2	6.5E-04
orf19.4192	*CDC14*	232.73	48.75	-2.3	2.8E-02
orf19.3967	*PFK1*	1129.72	236.63	-2.3	3.2E-03
orf19.655	*PHO84*	814.54	170.44	-2.3	1.9E-02
orf19.2724		211.55	43.68	-2.3	7.5E-03
orf19.1617		203.45	41.89	-2.3	5.2E-03
orf19.5877		665.62	136.78	-2.3	3.4E-04
orf19.7450		210.61	43.21	-2.3	1.1E-04
orf19.7254		212.34	43.52	-2.3	1.9E-04
orf19.1133	*MSB1*	232.83	47.44	-2.3	4.8E-05
orf19.6414		234.29	47.71	-2.3	1.5E-05
orf19.5372		1994.33	406.04	-2.3	2.8E-02
orf19.4076	*MET10*	373.72	75.64	-2.3	3.9E-05
orf19.3728		344.00	68.76	-2.3	2.3E-04
orf19.4712	*FGR6-3*	243.90	48.06	-2.3	4.5E-03
orf19.3211	*RCF3*	440.08	86.65	-2.3	8.5E-03
orf19.5406		776.40	152.72	-2.3	8.9E-03
orf19.3487		206.57	40.33	-2.4	3.8E-02
orf19.4890	*CLA4*	609.07	118.73	-2.4	2.8E-05
orf19.3789	*RPL24A*	994.33	192.29	-2.4	2.3E-03
orf19.132	*ScSIF2*	282.25	53.96	-2.4	2.6E-04
orf19.6960		229.99	43.77	-2.4	2.6E-02
orf19.2374		1166.05	220.97	-2.4	3.0E-03
orf19.3447		646.09	122.31	-2.4	1.2E-02
orf19.7017	*YOX1*	206.09	38.90	-2.4	4.9E-04
orf19.3207	*CCN1*	248.32	46.72	-2.4	3.1E-04
orf19.3764	*GSG1*	240.36	45.11	-2.4	1.1E-02
orf19.3555	*BUD14*	211.38	39.59	-2.4	3.2E-03
orf19.580		1248.70	233.73	-2.4	1.5E-02
orf19.7272		418.26	78.22	-2.4	9.7E-04
orf19.914		272.21	50.89	-2.4	6.7E-04
orf19.2467	*PRN1*	260.22	48.48	-2.4	5.0E-04
orf19.173		446.49	82.60	-2.4	2.9E-02
orf19.7506		235.88	43.56	-2.4	1.6E-04
orf19.985		474.61	87.59	-2.4	1.6E-04
orf19.6276		436.39	80.40	-2.4	2.7E-03
orf19.1409	*VAC7*	233.22	42.58	-2.5	1.3E-04
orf19.3624	*ScDSS1*	210.32	38.25	-2.5	1.4E-03
orf6.2737		262.92	47.05	-2.5	1.3E-03
orf19.5292	*AXL2*	498.94	88.86	-2.5	9.9E-05
orf19.2641	*ARP1*	441.08	78.14	-2.5	5.2E-04
orf19.2608	*ADH5*	38.02	6.67	-2.5	5.0E-02
orf19.2680	*ScDNF3*	546.73	95.12	-2.5	4.4E-04
orf19.3622	*ANP1*	290.44	50.36	-2.5	6.0E-03
orf19.6686	*ENP2*	1002.10	173.09	-2.5	6.4E-06

orf19.3820		218.27	37.27	-2.6	6.1E-03
orf19.3089		484.42	82.28	-2.6	1.3E-03
orf19.5518		572.37	96.50	-2.6	8.2E-05
orf19.2372		928.93	156.31	-2.6	7.1E-03
orf19.3469		371.38	62.47	-2.6	6.1E-03
orf19.1119	*MTR10*	298.82	50.06	-2.6	4.9E-04
orf19.4365		830.24	139.05	-2.6	8.1E-05
orf6.279		1568.85	261.70	-2.6	2.1E-03
orf19.3144		270.44	44.67	-2.6	6.7E-04
orf19.5531	*CDC37*	406.64	66.93	-2.6	3.8E-03
orf19.4552		550.39	90.48	-2.6	5.0E-04
orf19.4284	*BUR2*	238.06	39.08	-2.6	1.6E-05
orf19.2827		310.53	50.90	-2.6	6.1E-03
orf19.2236		306.91	50.24	-2.6	2.9E-03
orf19.946	*MET14*	394.41	64.24	-2.6	4.7E-03
orf19.1351		205.74	33.43	-2.6	2.6E-04
orf19.7359	*CRZ1*	309.84	49.73	-2.6	3.1E-05
orf19.564	*KAR3*	269.41	43.03	-2.6	2.8E-03
orf19.4276		266.44	42.42	-2.7	3.3E-05
orf6.1533	*CDC39*	1021.42	162.41	-2.7	1.1E-03
orf19.3345	*SIZ1*	289.83	44.90	-2.7	6.2E-04
orf19.4365		663.84	102.14	-2.7	1.1E-03
orf19.1666		253.45	38.96	-2.7	8.5E-04
orf19.5280	*MUP1*	660.51	98.83	-2.7	7.2E-03
25S.6.3p	*N/A*	2066.83	309.08	-2.7	4.6E-02
orf19.68		423.42	63.31	-2.7	2.9E-03
orf19.6514	*CUP9*	323.39	48.20	-2.7	2.5E-03
orf19.4722		309.70	44.97	-2.8	3.4E-03
orf19.5755		291.21	42.26	-2.8	4.4E-04
orf19.6537		231.79	32.73	-2.8	6.0E-03
orf19.4643		263.80	36.29	-2.9	5.6E-03
orf19.1383		201.85	27.60	-2.9	2.5E-03
orf19.2028	*MXR1*	1632.44	222.54	-2.9	2.9E-03
orf19.4952		647.02	87.72	-2.9	2.4E-03
orf19.6978		244.63	33.09	-2.9	3.9E-03
orf6.4835		439.29	58.84	-2.9	3.5E-03
orf19.414		274.37	36.51	-2.9	1.7E-04
orf19.660		278.97	36.90	-2.9	1.8E-04
orf19.3111	*PRA1*	449.24	58.86	-2.9	4.2E-05
orf19.422	*SPT20*	224.95	29.41	-2.9	1.9E-03
orf19.3148		602.75	77.88	-3.0	5.5E-04
orf19.5953		569.52	73.11	-3.0	7.2E-05
orf19.4553		335.99	43.10	-3.0	1.0E-04
orf19.1479		432.98	55.50	-3.0	2.0E-04
orf19.4912		234.89	30.08	-3.0	4.1E-03
orf19.522		1516.38	193.77	-3.0	1.8E-04
orf19.5528	*MOB1*	1124.01	143.39	-3.0	8.1E-04
orf19.6209		1201.19	153.15	-3.0	5.8E-03
orf19.3202		268.62	34.18	-3.0	4.5E-05
orf19.3840		442.03	55.67	-3.0	6.5E-06
orf6.1268		1505.45	188.98	-3.0	1.4E-03
orf19.4666		887.20	108.32	-3.0	1.0E-03
orf19.3142		287.08	34.62	-3.1	2.8E-03
orf19.267		943.48	113.24	-3.1	3.0E-03
orf19.2550		1797.45	214.88	-3.1	4.2E-03
orf19.5056		85.29	9.97	-3.1	2.3E-02

orf6.3626		1478.49	172.21	-3.1	1.2E-03
orf19.4347		280.17	32.17	-3.1	3.0E-04
orf19.1555	*SAC3*	1566.52	179.34	-3.1	3.2E-03
orf19.3603		984.41	111.29	-3.1	6.6E-04
orf19.4741		1243.92	139.75	-3.2	1.8E-03
orf19.3956		2761.71	304.61	-3.2	4.0E-04
orf19.5645	*MET15*	994.34	109.00	-3.2	4.9E-03
orf19.750		1506.08	159.66	-3.2	4.6E-03
orf19.1353		1922.26	203.26	-3.2	1.5E-03
orf19.6309		880.34	93.02	-3.2	4.0E-03
orf19.1960	*CLN3*	303.77	30.57	-3.3	6.1E-03
orf19.4750		309.87	29.88	-3.4	9.0E-05
orf19.156	*FGR51*	259.83	23.70	-3.5	7.7E-04
orf19.176	*OPT4*	1212.63	110.14	-3.5	4.6E-03
orf19.4699		1255.18	113.67	-3.5	1.2E-03
orf19.6981		237.14	21.04	-3.5	5.8E-05
orf19.5842		596.72	52.35	-3.5	2.8E-03
orf19.1960	*CLN3*	914.76	77.71	-3.6	6.4E-03
orf19.3563		245.46	20.69	-3.6	1.1E-03
orf19.4322	*DAP2*	278.76	22.18	-3.7	2.0E-03
orf19.2555	*URA5*	1160.78	90.13	-3.7	1.0E-03
orf19.1868	*RNR22*	123.73	9.60	-3.7	5.2E-03
orf19.177		267.06	20.33	-3.7	2.5E-05
orf19.843		1387.07	102.46	-3.8	1.4E-04
orf19.3695		858.38	60.32	-3.8	4.9E-03
orf6.2920		1559.11	104.55	-3.9	2.6E-03
orf19.5742	*ALS9*	1606.72	105.02	-3.9	2.0E-03
orf6.4638		219.69	11.73	-4.2	1.7E-06
orf19.1995	*ScMNN2*	266.12	13.48	-4.3	6.1E-05
orf6.2374		338.80	17.03	-4.3	7.0E-04
orf19.3869		1808.51	87.68	-4.4	3.0E-05
orf19.334		468.07	10.90	-5.4	1.5E-03

Supplementary Table 2. Bioactive lipids present on the array.

Name	Conc.	MW
5(S)-HETE	0.1mM	320.2
(±)5-HETE	0.1mM	320.2
(±)5-HETE LACTONE	0.1mM	302.2
8(S)-HETE	0.1mM	320.2
9(S)-HETE	0.1mM	320.2
EMPTY		
12(S)-HETE	0.1mM	320.2
12(R)-HETE	0.1mM	320.2
15(S)-HETE	0.1mM	320.2
15(S)-HEDE	0.1mM	324.3
(±)5-HETrE	0.1mM	322.3
TETRANOR-12(R)-HETE	0.1mM	266.2
15(S)-HETrE	0.1mM	322.3
(±)5-HEPE	0.1mM	318.2
15(S)-HEPE	0.1mM	318.2
5(S)-HPETE	0.1mM	336.2
12(S)-HPETE	0.1mM	336.2
15(S)-HPETE	0.1mM	336.2

15(S)-HPEDE	0.1mM	340.3
15(S)-HPEPE	0.1mM	334.2
(±)4-HYDROXYNON-2-ENAL	1mM	156.1
HEPOXILIN A3	0.1mM	336.2
HEPOXILIN B3	0.1mM	336.2
12(S),20-DIHETE	0.1mM	336.2
5(S),15(S)-DIHETE	0.1mM	336.2
8(S),15(S)-DIHETE	0.1mM	336.2
5(S),6(R)-DIHETE	0.1mM	336.2
5(S),12(R)-DIHETE all trans	0.1mM	336.2
8(R),15(S)-DIHETE all trans	0.1mM	336.2
5(S),12(S)-DIHETE all trans	0.1mM	336.2
8(S),15(S)-DIHETE all trans	0.1mM	336.2
5,6-EPOXYEICOSATRIENOIC ACID	0.1mM	320.2
8,9-EPOXYEICOSATRIENOIC ACID	0.1mM	320.2
11,12-EPOXYEICOSATRIENOIC ACID	0.1mM	320.2
14,15-EPOXYEICOSATRIENOIC ACID	0.1mM	320.2
5-KETOEICOSATETRAENOIC ACID	0.1mM	318.2
15-KETOEICOSATETRAENOIC ACID	0.1mM	318.2
13-KETOOCTADECADIENOIC ACID	0.1mM	294.2
LEUKOTRIENE B3	0.1mM	338.2
LEUKOTRIENE B4	0.1mM	336.2
20-HYDROXY-LEUKOTRIENE B4	0.1mM	352.2
20-CARBOXY-LEUKOTRIENE B4	0.1mM	366.2
LEUKOTRIENE C4	0.1mM	625.3
LEUKOTRIENE D4	0.1mM	496.3
LEUKOTRIENE E4	0.1mM	439.2
N-ACETYL-LEUKOTRIENE E4	0.1mM	481.2
LIPOXIN A4	0.1mM	352.2
EPOXY-OLEIC ACID	0.1mM	298.3
PROSTAGLANDIN A1	1mM	336.2
PROSTAGLANDIN A2	1mM	334.2
PROSTAGLANDIN B1	1mM	336.2
PROSTAGLANDIN B2	1mM	334.2
PROSTAGLANDIN D2	1mM	352.2
PROSTAGLANDIN E1	1mM	354.2
PROSTAGLANDIN E2	1mM	352.2
PROSTAGLANDIN F2a	1mM	354.2
PROSTAGLANDIN F1a	1mM	356.3
PROSTAGLANDIN I2 Na	1mM	352.2
15-KETO-PROSTAGLANDIN E2	1mM	350.2
15-KETO-PROSTAGLANDIN F2a	1mM	352.2
13,14-DIHYDRO-15-KETO-PGF2a	1mM	354.2
6-KETO-PROSTAGLANDIN F1a	1mM	370.2
16,16-DIMETHYL-PROSTAGLANDIN E2	1mM	380.3
U-46619	1mM	350.2
9b,11a PROSTAGLANDIN F2	1mM	354.2
9a,11b PROSTAGLANDIN F2	1mM	354.2
PROSTAGLANDIN J2	1mM	334.2
2,3-DINOR-6-KETO-PGF1a	0.1mM	342.2
CARBACYCLIN	1mM	350.2
(±)13-AZAPROSTANOIC ACID	1mM	311.3
19(R)-HYDROXY-PROSTAGLANDIN E2	1mM	368.2
19(R)-HYDROXY-PROSTAGLANDIN F2a	0.1mM	370.2

17-PHENYL-TRINOR-PGE2	1mM	386.2
D12-PROSTAGLANDIN J2	1mM	334.2
13,14-DIHYDRO-PGE1	1mM	356.3
8-EPI-PROSTAGLANDIN F2a	1mM	354.2
15d-PGJ2	1mM	316.2
MISOPROSTOL, FREE ACID	1mM	368.3
THROMBOXANE B2	1mM	370.2
11-DEHYDRO-THROMBOXANE B2	1mM	368.2
ANANDAMIDE (20:4, n-6)	1mM	347.3
PALMITYLETHANOLAMIDE	1mM	299.3
ANANDAMIDE (18:2,n-6)	1mM	323.3
ANANDAMIDE (20:3,n-6)	1mM	349.3
ANANDAMIDE (22:4,n-6)	1mM	375.3
MEAD ETHANOLAMIDE	1mM	349.3
(R)-METHANANDAMIDE	1mM	361.3
BML-190	1mM	426.1
N-Arachidonylglycine	1mM	361.3
EMPTY		
WIN 55,212-2	1mM	426.2
ARACHIDONAMIDE	1mM	303.3
LINOLEAMIDE	1mM	279.3
9,10-OCTADECENOAMIDE	1mM	281.3
ACETYL-FARNESYL-CYSTEINE	1mM	367.2
S-FARNESYL-L-CYSTEINE ME	1mM	339.2
AGGC	1mM	435.3
AGC	1mM	299.2
FARNESYLTHIOACETIC ACID	1mM	296.2
9(S)-HODE	0.1mM	296.2
(±)9-HODE	0.1mM	296.2
13(S)-HODE	0.1mM	296.2
(±)13-HODE	0.1mM	296.2
13(S)-HOTE	0.1mM	294.2
9(S)-HPODE	0.1mM	312.2
13(S)-HPODE	0.1mM	312.2
LEUKOTOXIN A (9,10-EODE)	0.1mM	296.2
LEUKOTOXIN B (12,13-EODE)	0.1mM	296.2
12(S)-HHT	0.1mM	280.2
25-HYDROXYVITAMIN D3	1mM	400.3
1,25-DIHYDROXYVITAMIN D3	1mM	416.3
24,25-DIHYDROXYVITAMIN D3	1mM	416.3
RETINOIC ACID, ALL TRANS	1mM	300.2
9-CIS RETINOIC ACID	1mM	300.2
13-CIS RETINOIC ACID	1mM	300.2
4-HYDROXYPHENYLRETINAMIDE	1mM	391.3
AM-580	1mM	351.2
TTNPB	1mM	348.2
METHOPRENE ACID	1mM	268.2
WY-14643	1mM	323.0
CIGLITAZONE	1mM	333.1
CLOFIBRATE	1mM	242.1
5,8,11-EICOSATRIYNOIC ACID	1mM	300.2
5,8,11,14-EICOSATETRAYNOIC ACID	1mM	296.2
1,2-DIDECANOYL-GLYCEROL (10:0)	1mM	400.3
1,2-DIOCTANOYL-SN-GLYCEROL	1mM	344.3

1,2-DIOLEOYL-GLYCEROL (18:1)	1mM	620.5
1-OLEOYL-2-ACETYL-GLYCEROL	1mM	398.3
1-STEAROYL-2-ARACHIDONOYL-GLYCEROL	1mM	644.5
RICINOLEIC ACID	1mM	298.3
1-HEXADECYL-2-ARACHIDONOYL-GLYCEROL	1mM	602.5
1-HEXADECYL-2-O-METHYL-GLYCEROL	1mM	330.3
1-HEXADECYL-2-O-ACETYL-GLYCEROL	1mM	358.3
2,3-DINOR-THROMBOXANE B2	0.1mM	342.2
14,15-DEHYDRO-LEUKOTRIENE B4	0.1mM	334.2
REV-5901	1mM	335.2
LY-171883	1mM	318.2
U-75302	0.1mM	361.3
SQ-29548	1mM	387.2
FLUPROSTENOL	1mM	458.2
CLOPROSTENOL Na	1mM	424.2
EICOSAPENTAENOIC ACID (20:5 n-3)	1mM	302.2
DOCOSAHEXAENOIC ACID (22:6 n-3)	1mM	328.2
ARACHIDONIC ACID (20:4 n-6)	1mM	304.2
MEAD ACID (20:3 n-9)	1mM	306.3
LINOLENIC ACID (18:3 n-3)	1mM	278.2
GAMMA-LINOLENIC ACID (18:3 n-6)	1mM	278.2
EICOSA-5,8-DIENOIC ACID (20:2 n-12)	1mM	308.3
EICOSADIENOIC ACID (20:2 n-6)	1mM	308.3
7,7-DIMETHYLEICOSADIENOIC ACID	1mM	336.3
EICOSATRIENOIC ACID (20:3 n-3)	1mM	306.3
DIHOMO-GAMMA-LINOLENIC ACID	1mM	306.3
DOCOSATRIENOIC ACID (22:3 n-3)	1mM	334.3
ADRENIC ACID (22:4 n-6)	1mM	332.3
DOCOSAPENTAENOIC ACID	1mM	330.3
LINOLEIC ACID	1mM	280.2
17-OCTADECYNOIC ACID	1mM	280.2
2-HYDROXYMYRISTIC ACID	1mM	244.2
2-FLUOROPALMITIC ACID	1mM	274.2
4-OXATETRADECANOIC ACID	1mM	230.2
12-METHOXYDODECANOIC ACID	1mM	230.2
SPHINGOSINE	1mM	299.3
C2 CERAMIDE	1mM	341.3
C2 DIHYDROCERAMIDE	1mM	343.3
N,N-DIMETHYLSPHINGOSINE	1mM	327.3
C8 CERAMIDE	1mM	425.4
C8 DIHYDROCERAMIDE	1mM	427.4
C16 CERAMIDE	1mM	537.5
DIHYDROSPHINGOSINE	1mM	301.3
SPHINGOMYELIN *	100nmol	730.6
SPHINGOSINE-1-PHOSPHATE *	100nmol	379.2
SPHINGOSYLPHOSPHORYL CHOLINE *	100nmol	464.3
DIHYDROSPHINGOSINE-1-PHOSPHATE *	100nmol	381.3
C8 CERAMINE	1mM	411.4
DL-DIHYDROSPHINGOSINE	1mM	301.3
DL-PDMP	1mM	390.3
DL-PPMP	1mM	474.4
MAPP, D-erythro	1mM	361.3

MAPP, L-erythro	1mM	361.3
PAF C16	1mM	523.4
LYSO-PAF C16	1mM	481.4
PAF C18	1mM	551.4
LYSO-PAF C18 *	100nmol	509.4
PAF C18:1	1mM	549.4
ENANTIO-PAF C16	1mM	523.4
ARACHIDONOYL-PAF	1mM	767.6
2-EPA-PAF	1mM	751.6
2-DHLA-PAF	1mM	769.6
DCHA-PAF	1mM	791.6
1-HEXADECYL-2-METHYLGLYCERO-3 PC	1mM	495.4
1-OCTADECYL-2-METHYLGLYCERO-3 PC	1mM	523.4
C-PAF	1mM	538.4
1-ACYL-PAF	1mM	537.3
LYSOPHOSPHATIDIC ACID	1mM	436.3
L-NASPA	1mM	423.2
PHOSPHATIDIC ACID, DIPALMITOYL	1mM	648.5
AM251	1mM	554.0
2-ARACHIDONOYLGLYCEROL	1mM	378.3
6-FORMYLINDOLO [3,2-B] CARBAZOLE	1mM	284.1
DIINDOLYLMETHANE	1mM	246.1
N-LINOLEOYLGLYCINE	1mM	337.3
PALMITOYL DOPAMINE	1mM	391.3
OLEOYL DOPAMINE	1mM	417.3
ARACHIDONOYL DOPAMINE	1mM	439.3

Supplementary Table 3. Yeast strains used in this study

Name	Genotype	Source
CaLC238	SN87, derivative of SC5314 leu2Δ/leu2Δ his1Δ/his1Δ URA3/ura3::imm434 IRO1/iro1::imm434	Noble
CaEL1 (wild type)	Isogenic to SN87, except his1::CdHIS1/his1Δ leu2::CmLEU2/leu2Δ	This study
CaLC941 (*orf19.633*Δ/Δ)	Isogenic to SN87, except orf19.633::CdHIS1/orf19.633::CmLEU2	Gift from Leah Cowen
*sld1*Δ/Δ	Isogenic to CaEL1, except sld1Δ/sld1::CaNAT	This study
*mts1*Δ/Δ	Isogenic to CaEL1, except mts1Δ/mts1::CaNAT	This study
*orf19.752*Δ/Δ	Isogenic to CaEL1, except orf19.752Δ/orf19.752::CaNAT	This study
*hsx11*Δ/Δ	Isogenic to CaEL1, except hsx11Δ/hsx11::CaNAT	This study
*sld1*Δ/Δ *orf19.633*Δ/Δ	Isogenic to CaLC941, except sld1Δ/sld1::CaNAT	This study
*mts1*Δ/Δ	Isogenic to CaLC941, except	This study

*orf19.633*Δ/Δ	mts1Δ/mts1::CaNAT	
*orf19.752*Δ/Δ	Isogenic to CaLC941, except	This study
*orf19.633*Δ/Δ	orf19.752Δ/orf19.752::CaNAT	
*hsx11*Δ/Δ	Isogenic to CaLC941, except	This study
*orf19.633*Δ/Δ	hsx11Δ/hsx11::CaNAT	
BY4743	MATa/α his3Δ1/his3Δ1 leu2Δ0/leu2Δ0 LYS2/lys2Δ0	Brachmann
(wild-type)	met15Δ0/MET15 ura3Δ0/ura3Δ0	
*crg1*Δ/Δ	Isogenic to BY4743, except for crg1::KanMX	Giaever
	crg1::KanMX	

Brachmann CB, Davies A, Cost GJ, Caputo E, Li J, *et al.* (1998) Designer deletion strains derived from *Saccharomyces cerevisiae* S288C: a useful set of strains and plasmids for PCR-mediated gene disruption and other applications. Yeast 14: 115-132.
Giaever G, Chu AM, Ni L, Connelly C, Riles L, *et al.* (2002) Functional profiling of the *Saccharomyces cerevisiae* genome. Nature 418: 387-391.
Noble SM, Johnson AD (2005) Strains and strategies for large-scale gene deletion studies of the diploid human fungal pathogen Candida albicans. Eukaryot Cell 4: 298-309.

Supplementary Table 4. Plasmids used in this study

Plasmid name	Description	Source
pJK863 (pLC49)	FLP-CaNAT, ampR	Shen
pUC57	With optimized sequence orf19.633, AmpR	This study
BG1805	2 μm, URA3, GAL1prom, triple affinity tag (His6-HAepitope-3Cprotease site-ZZproteinA) at C-terminal	Lissina
orf19.633	As BG1805, with orf19.633	This study
D48A	As BG1805, orf19.633–D48A	This study
E153A/R156G	As BG1805 orf19.633–E153A/R156G	This study
Motif III Δ	As BG1805 orf19.633–Motif III Δ	This study

Supplementary Table 5. Primers used in this study

Primer name	Purpose	Oligonucleotide sequence (5'-3')
orf19.633 (mid)_F	qRT-PCR	ATCACCGGTGGAGAAATACG
orf19.633 (mid)_R	qRT-PCR	TGATTCATATCCTGCTTCTAATGC
ACT1 (3')_F	qRT-PCR	AGGTTTGGAAGCTGCTGGTA
ACT1 (3')_R	qRT-PCR	AGCAATACCTGGGAACATGG

D48A_F	Orf19.633 mutagenesis	TTCAAGATTTTAGCTGTTGGGTGCGGTCCTGG
D48A_R	Orf19.633 mutagenesis	GTTTGGTTTTATCAGTGGAATGACGTACTTAGC
E153A/R156G_F	Orf19.633 mutagenesis	GAAGCCTTGAAGGCATTGAAAGGAGTTACGAAACCAG
E153A/R156G_R	Orf19.633 mutagenesis	GATTGGATTCTGTAAATGAATGATCACCTGG
Motif III_F	Orf19.633 mutagenesis	ATCTGTATTAGAGATGCAGATTTGGAATCTAGTATAG
Motif III_R	Orf19.633 mutagenesis	CAGTTCATAGATAGAACCAATTTGAAACGAAATATTAGTC
MTS1_F	Double mutant construction	GTTTTCGTCTTTTGTCGAGTTTAACATTTCAATTGAATATCAATTTTTGTAACAATGCGTATGTTGTGTGGAATTGTGAG
MTS1_R	Double mutant construction	TATTCAGATCAGAATAAATAAAAATCTATACAAATACACCATAAAAGCTCAACCAGTTTAGGCGATTAAGTTGGGTAACG
SLD1_F	Double mutant construction	TTATTTATTTATTGTTATTTTTTTTTTTCACCTTCGTTAACAAACCTTTATGAGATAAACCATGCGTATGTTGTGTGGAATTGTGAG
SLD1_R	Double mutant construction	GTCTCTATATATATATCTATACCCTCATATAAATTTGCATAAAAGTTAAGAAAACAGGATACTGTCTAGGCGATTAAGTTGGGTAACG
HSX11_F	Double mutant construction	TACATTTGATCTTGTTTCTTTTATCAACACTGTGAAATATCGTAATCTTTTGTTCTTCTTTCTAATGCGTATGTTGTGTGGAATTGTGAG
HSX11_R	Double mutant construction	TTACATTTAACTTTTACTTATCTATATATACATGTCCTGTCTATCTATCTATAACAATTGGCGTATCAGGCGATTAAGTTGGGTAACG
orf19.752_F	Double mutant construction	TTCTTTGTATTATTGGTTAGATTTCCATTCCATATACACACAAGATGCGTATGTTGTGTGGAATTGTGAG
orf19.752_R	Double mutant construction	TTGAAGTGAGTTGATGTAGTAAATTATGTATGAATGTATATAAACCCTCAGGCGATTAAGTTGGGTAACG
confirm_Flip_NAT_F	Confirmation	CAACCACAAATGACCAGCAC
confirm_Flip_NAT_R	Confirmation	GTGATTTGGCTGGTTTCGTT
confirm_MTS1_F	Confirmation	CACATTTGCCCATCACTCTG
confirm_MTS1_R	Confirmation	CGAAGTCATGTTCGTGCATC
confirm orf19.752_F	Confirmation	CAAGCCGAGTCGGAAAACTA
confirm orf19.752_R	Confirmation	TGTGTTCGACACATCCTGGT
confirm_HSX11_F	Confirmation	TCGAACTGTCATCCTGTCCA
confirm_HSX11_R	Confirmation	TACAACCAAGCTGCGAAAAA

confirm_SLD1_F	Confirmation	CTTTTGGCAGGATTCTTGGA
confirm_SLD1_R	Confirmation	CCAAAAGAACCAGAGCTTGC
confirm_SLD1_1100bp_F	Confirmation	TGGACGTTGATTGTCCTGAA
confirm_HSX11_430bp_F	Confirmation	AATCGATTGGAGGGGAAGAC
confirm_MTS1_990bp_F	Confirmation	AGAGACGCTTTGGAAGACGA
confirm_orf19.752_995bp_F	Confirmation	CGACCTAATTGTTGCCAAGG
GAL1_orf19.633_F	*19.633* cloning	TTAACGTCAAGGAGAAGGAATTATCAAGTTTGTACAATGAGCGGTGCTAACAACAACCATCAAGTG
Cterm_orf19.633_R	*19.633* cloning	ATGGTGATGATGATGTCTAGACACATCAACCACTTTTGTACACACTTGACGTGTAGTTGTTGGTTTTTGGTA

Supplementary Figure 1

A

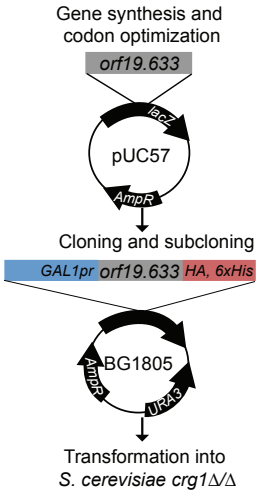

B

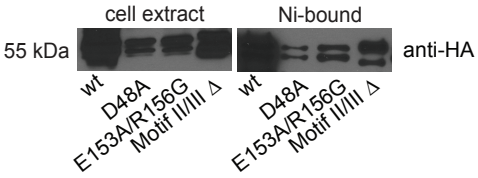

Supplementary Figure 2

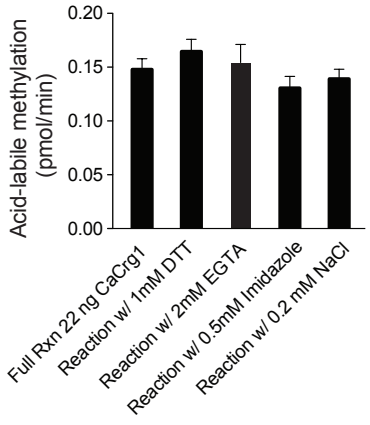

Supplementary Figure 3

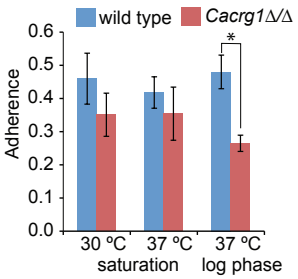

Supplementary Figure 4

A

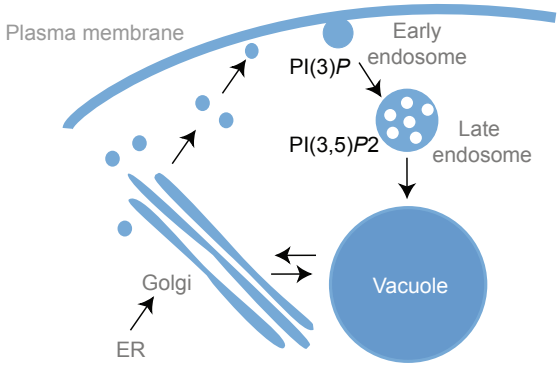

B

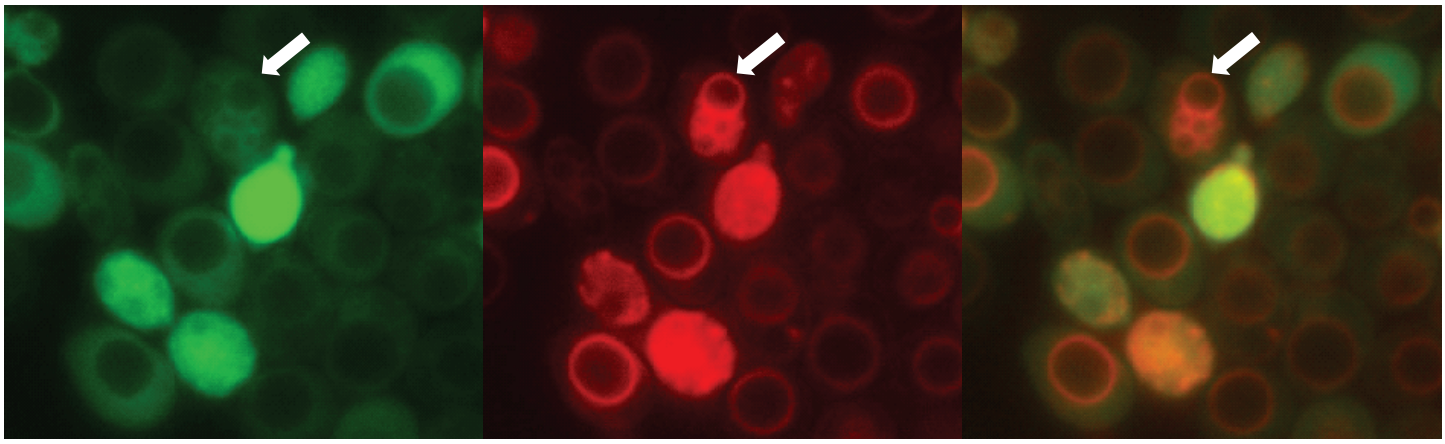

Supplementary Figure 5

A

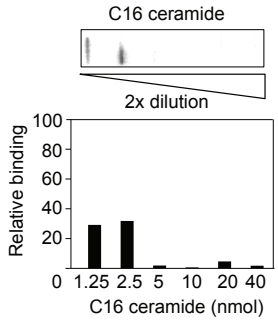

B

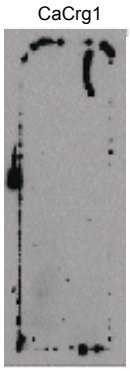

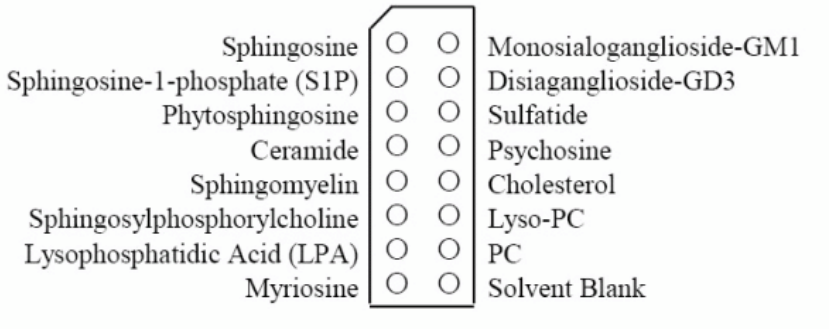

Supplementary Figure 6